doi.org/10.1002/hlca.202100085

COMMUNICATION

HELVETICA chimica acta

Inhibition of Thiol-Mediated Uptake with Irreversible Covalent Inhibitors

Bumhee Lim[+,a,b] Yangyang Cheng[+,a,b] Takehiro Kato[+,a,b] Anh-Tuan Pham,[a,b] Eliott Le Du,[c] Abhaya Kumar Mishra,[b,c] Elija Grinhagena,[b,c] Dimitri Moreau,[b] Naomi Sakai,[a,b] Jerome Waser,*[b,c] and Stefan Matile*[a,b]

[a] Department of Organic Chemistry, University of Geneva, Quai Ernest Ansermet 30, CH-1211 Geneva 4, Switzerland, e-mail: stefan.matile@unige.ch

[b] National Centre of Competence in Research (NCCR) Chemical Biology, Quai Ernest Ansermet 30, CH-1211 Geneva 4, Switzerland

[c] Laboratory of Catalysis and Organic Synthesis, Ecole Polytechnique Fédérale de Lausanne EPFL SB ISIC LCSO, BCH 4306, 1015 Lausanne, Switzerland, e-mail: jerome.waser@epfl.ch

Dedicated to *Peter Kündig* on the occasion of his 75th birthday

Thiol-mediated uptake is emerging as method of choice to penetrate cells. This study focuses on irreversible covalent inhibitors of thiol-mediated uptake. High-content high-throughput screening of the so far largest collection of hypervalent iodine reagents affords inhibitors that are more than 250 times more active than *Ellman*'s reagent and rival the best dynamic covalent inhibitors. Comparison with other irreversible reagents reveals that inhibition within one series follows reactivity, whereas inhibition across series deviates from reactivity. These trends support that molecular recognition, besides dynamic covalent exchange, contributes significantly to thiol-mediated uptake. The most powerful inhibitors besides the best hypervalent iodine reagents were *Fukuyama*'s nosyl protecting group and super-cinnamaldehydes that have been introduced as irreversible activators of the pain receptor TRPA1. Considering that several viruses use different forms of thiol-mediated uptake to enter cells, the identification of new irreversible inhibitors of thiol-mediated uptake is of general interest for the discovery of new antivirals.

Keywords: antiviral agents, hypervalent compounds, hypervalent iodine reagents, inhibitors, nosyl protecting group, thiol-mediated uptake, TRPA1 pain receptor.

Thiol-mediated uptake is an intriguing process because it works so well but is so poorly understood.[1] The ability of oligochalcogenides, usually disulfides, to facilitate cell penetration has been observed in many variations.[2–14] The unifying theme is dynamic covalent oligochalcogenide exchange with thiols (and/or disulfides) on the cell surface that can be inhibited by thiol reactive agents (*Figure 1,a*). This central dynamic covalent chemistry process can be coupled to diverse uptake mechanisms, including endocytosis, fusion and also direct translocation across the plasma membrane directly into the cytosol.

Early examples on thiol-mediated uptake focus mainly on the entry of viruses into cells. Particular emphasis has been on HIV, which proceeds by fusion after the essential dynamic-covalent exchange with protein disulfide isomerases on cell surfaces.[15] More recently, privileged scaffolds such as CPDs (cell-penetrating poly(disulfide)s) and COCs (cyclic oligochalcogenides)[16] have been introduced to exploit thiol-mediated uptake for the efficient delivery of

[+] These authors contributed equally to this study.

Supporting information for this article is available on the WWW under https://doi.org/10.1002/hlca.202100085

a broad variety of substrates into the cytosol.[1] This includes substrates that are significant and, depending on the context, often problematic to deliver otherwise, *e.g.*, antibodies,[4] DNA/RNA, nanoparticles,[7] artificial enzymes,[17] quantum dots,[18] liposomes and polymersomes.[19]

Ellman's reagent has been the benchmark inhibitor to probe for thiol-mediated uptake until recently.[20] This choice has not been beneficial for the field, because 5,5′-dithio-bis(2-nitrobenzoic acid) (DTNB) is a notoriously weak and unreliable inhibitor. The poor performance of *Ellman*'s reagent is reasonable considering that it produces activated disulfides on cell surfaces that readily continue to exchange. Together with challenges in target identification with dynamic networks,[1] unreliable DTNB data have helped to raise questions concerning significance, nature and even the very existence of thiol-mediated uptake. Earlier this year, these overall unnecessary questions have been addressed with a broad inhibitor screening.[20] Up to 5000 times more powerful inhibitors were found. In preliminary tests, a few of the identified inhibitors also inhibited the entry of SARS-CoV-2 spike pseudo-lentiviruses, with efficiencies clearly exceeding the popular ebselen[21,22] (mostly unpublished). It remains to be seen whether or not this is more than a coincidence. The same holds for the transferrin receptor (among many other possible targets), found in both proteomics screens for thiol-mediated uptake of COCs[23] as well as contributing to the entry of SARS-CoV-2.[24]

Inhibitor screening for thiol-mediated uptake has so far focused on dynamic covalent inhibitors.[20] The objective of this study was to shift attention to irreversible inhibition. Particular emphasis is on hypervalent iodine reagents of different structure and reactivity (*Figure 1,b*). Hypervalent iodine reagents centered around the ethynyl benziodoxolone (EBX) scaffold react with high rate with thiols.[25,26] They have been used previously in proteomics studies of the cysteinome, and excelled with unique reactivity and selectivity.[27] Other applications include further derivatizations of cysteines,[28,29] peptide Cys-Cys and Cys-Lys stapling,[30] functional terminators of CPDs,[31] and classical use as alkynylation reagents in organic synthesis.[32,33] The results from irreversible inhibition of thiol-mediated uptake with hypervalent iodine reagents are then compared to classical and modern irreversible thiol-reactive agents.[34–45] Hypervalent iodine reagents emerge top, together with *Fukuyama*'s nosyl protecting group[34] and super-cinnamaldehyde

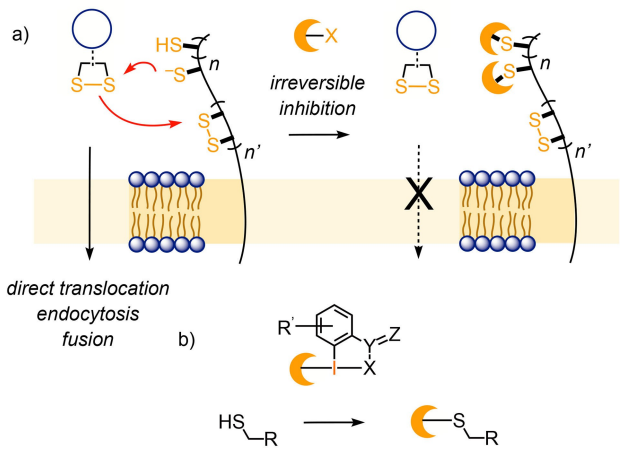

Figure 1. a) Thiol-mediated uptake operates with inhibitable dynamic covalent chalcogen exchange cascades before or during cellular entry by direct translocation, endocytosis or fusion, usually thiol/disulfide exchange. b) General scheme for inhibition with irreversible covalent inhibitors.

ligands of the pain receptor TRPA1,[35] all rivaling the best reversible inhibitors.

The inhibitor candidates **1**–**25** tested in this study were numbered to roughly reflect their identified activity, decreasing with increasing numbers, with DTNB ending up as number **25** (*Figure 2*). They were synthesized mostly following reported procedures (see *Supporting Information*).

For inhibitor screening of thiol-mediated uptake, the conjugate **26** composed of an epidithiodiketopiperazine (ETP), *i.e.*, one of the most active COCs,[46] and fluorescein (FITC) was used as reporter (*Figure 3*). FITC-ETP **26** rapidly penetrates unmodified HeLa cells to end up staining cytosol and nucleus.[46] In this assay, inhibition of thiol-mediated uptake is detected as decreasing fluorescence of the cells (*Figure 3*). For inhibitor screening, a recently introduced fully automated, fluorescent microscopy image-based high-content high-throughput screening (HCHTS) was used.[20,47] Namely, HeLa cells in multiwell plates were incubated first with inhibitor candidates for a given period of time. Then, reporter **26** was added to penetrate cells within 30 minutes. Afterward, the multiwell plates were washed to remove all reporter and inhibitor candidates in the media, *Hoechst 33342* and propidium iodide were added for automated analysis, and the CSLM images were recorded. *Hoechst 33342* is a cell-permeable DNA stain applied to stain all cells, propidium iodide is a cell-impermeable DNA stain used to differentiate necrotic and apoptotic from healthy cells. Relative cell viability (*RV*) was calculated

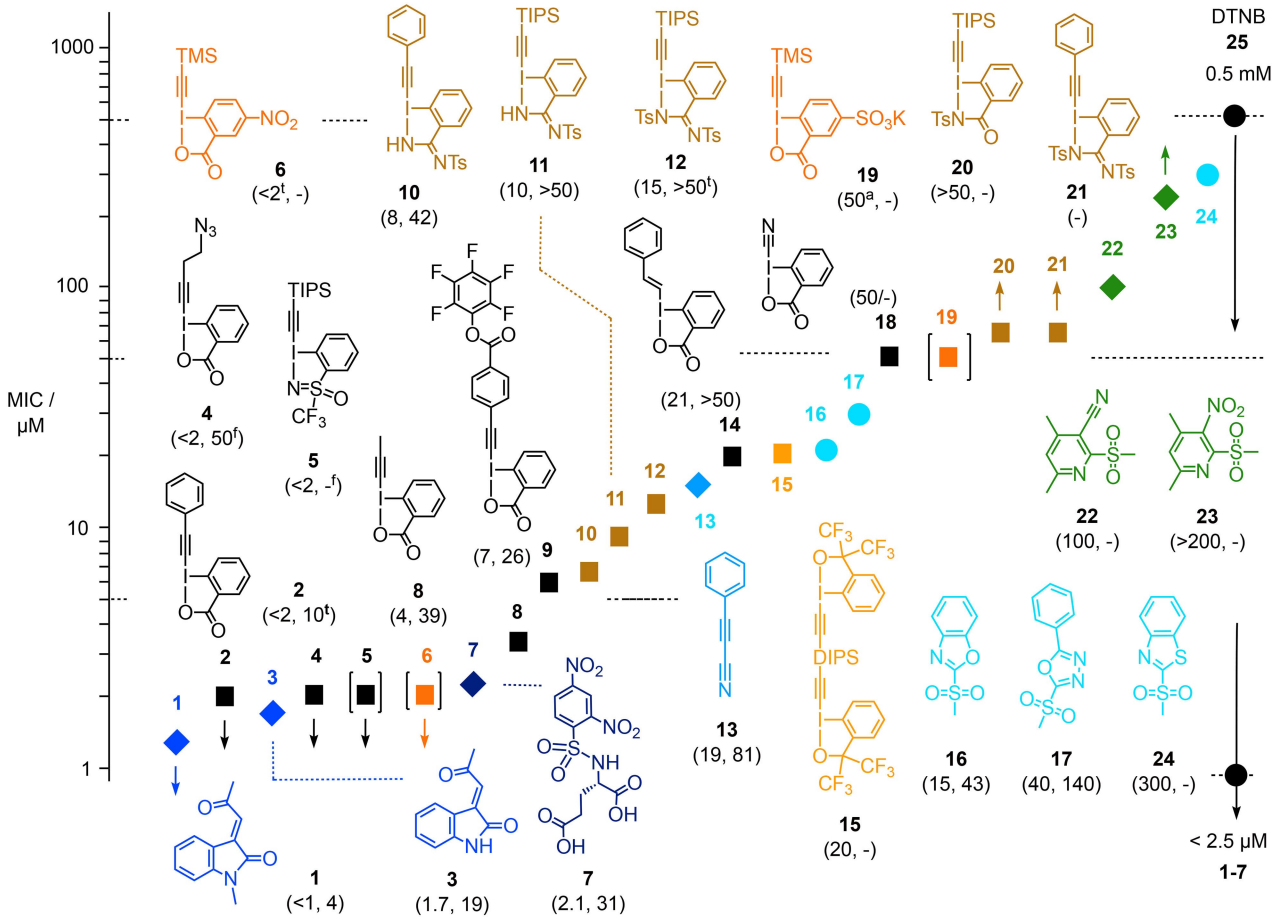

Figure 2. Structure of inhibitor candidates **1**–**24** with their concentrations needed to inhibit by *ca.* 15% (MIC) the thiol-mediated uptake of fluorescently-labeled ETP **26**. All results were obtained by 1 h pre-incubation of HeLa cells with inhibitor candidates, followed by 30 min incubation with reporter **26**. Below compound numbers are given, in parenthesis, first MIC, then, if detectable, IC_{50}, both in µM. t, onset of toxicity; f, 'flat' dose-response curve (see text); a, onset of activation of uptake; upward arrows, MIC not reached at indicated concentration; downward arrows, MIC already passed at indicated concentration (compare dose response curves, *Figures 4*, *S1*–*S4*). MIC values indicated by symbols in brackets are approximate.

automatically from the ratio of propidium iodide and *Hoechst 33342* labeled cells (*Figure 4*; results were backed up with MTT cell viability assays for selected inhibitors, *Figure S5*). Propidium iodide negative cells were kept to determine average fluorescence intensity from reporter **26** for intact cells only. This fully automated procedure was important to secure quantitative data on both uptake and toxicity, and to record uptake independent from toxicity. In other words, uptake data refer to intact cells exclusively, even at high toxicity.

In this assay, it is possible to remove inhibitor candidates from the media before reporter addition, a method referred to as 'pre-incubation' which, in principle, excludes direct interaction between reporter and inhibitor and thus limits inhibitor exchange to cellular target. The alternative addition of reporter without prior inhibitor removal is referred to as 'co-incubation' method, which, in principle, does not exclude direct interaction between reporter and inhibitors that have not reacted before with cellular targets.

The results of HCHT inhibitor screening were ranked according to their MIC, that is the minimal inhibitory concentration needed to inhibit the thiol-mediated uptake of FITC-ETP **26** by *ca.* 15% (*Figure 2*). MICs were preferable over IC_{50}'s, that is the concentration needed for 50% inhibition, because competing high concentration effects such as toxicity, precipitation or even activation, could produce highly unusual dose response curves (*Figure 4*). Such anomalous concentration dependence is also the origin of conflicting results with *Ellman*'s reagent **25**, which reaches MIC around 0.5 mM and loses this marginal activity

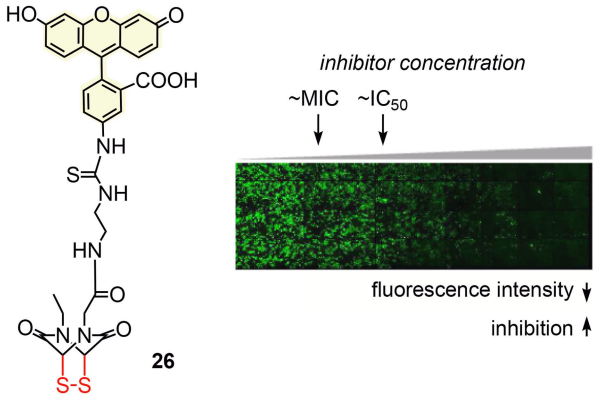

Figure 3. Structure of FITC-ETP reporter **26** and representative multiwell plate for automated HCHT inhibitor screening of HeLa Kyoto cells incubated first with, from left to right, increasing concentrations of an inhibitor and then with a constant concentration of **26**. Each green dot represents at least one HeLa cell penetrated by **26**, and the response in decreasing fluorescence of cells to increasing concentration characterizes the efficiency of the inhibitor, quantified in MIC and IC_{50}, see *Figure 2*.

again at higher concentrations due to the onset of weak uptake activation (*Figure 2*). Such uptake activation at high concentrations often indicates the onset of membrane damage and coincides with the onset of cytotoxicity (*Figures 4,i* and *4,j*).

The ability of hypervalent iodine reagents to inhibit thiol-mediated uptake varied enormously, covering the full range of MICs <2 μM to undetectable inhibition at >100 μM (*Figure 2*). In general, increasing inhibition activity coincided beautifully with increasing reactivity of the hypervalent iodine reagent. The most impressive MICs were obtained for the classical ethynyl benziodoxolone such as **2**, **4**, **6**, **8** and **9**.[26,27,29,30] Substitution of the terminal phenyl in ethynyl benziodoxolone **2** with a methyl in **8** reduced activity to MIC = 4 μM but improved dose response curve profiles with regard to toxicity at higher concentration (*Figures 2*, *4,a* and *4,e*).

Replacement of the benziodoxolone in **2** with a less reactive, *N*-stabilized benziodazolimine in **10**[48] caused the respective drop from MIC <2 μM to MIC = 8 μM, together with an attractive decrease in toxicity at higher concentrations (*Figures 2*, *4,b* and *4,e*). Tosylation of the second nitrogen in benziodazolimine **10** gave the completely inactive **21** with an MIC >100 μM (*Figures 2*, *4,b* and *4,c*).[48] This inactivation by tosylation was again consistent with the poor reactivity of **21**, which is caused by a halogen bond[49–52] from the tosyl oxygen acceptor to the hypervalent iodine donor (*Figure 5*).[48] Similar inactivation by intramolecular σ-hole interactions has already been observed for anion transport with chalcogen bonds[53] as well as catalysis with pnictogen bonds,[54] and used extensively in the design of fluorescent flipper probes.[53,55] Replacement of the terminal phenyl group with a TIPS gave the same trend with **11** and **12**, although clearly less pronounced (*Figure 2*). Benziodazolone **20** was inactive, whereas increasing reactivity with an activated benziodosulfoximine **5** afforded the expected low MIC <2 μM together with, however, an inacceptable dose response curve (*Figures 2*, *4,h*; *vide infra*).

Replacement of the alkyne in benziodoxolone **2** with an alkene in vinylbenziodoxolone[56] **14** reduced activity as expected from reduced reactivity (*Figures 2*, *4,d* and *4,e*). Similarly reduced activity of the highly reactive nitrile **18** is presumably due to instability in water. Activation of the benziodoxolone in **2** with a nitro acceptor in *para* position gave **6** with an excellent MIC <2 μM together with excessive toxicity (*Figures 2*, *4,e* and *4,g*). The anionic sulfonate acceptor in the analogous **19**[57] resulted in uptake activation rather than inhibition above 50 μM (*Figure 2*). Such activation often coincides with the onset of toxicity and has been attributed to membrane-disrupting detergent-like activity at higher concentration. This interpretation was in good agreement with the amphiphilic structure of the anion **19**.

The ethynyl benziodoxole dimer **15**, originally conceived for peptide stapling,[30] was attractive with regard to the recognition of neighboring thiols on the cell surface. However, the modest performance with MIC = 20 μM was dominated by the reduced reactivity rather than divalency (*Figure 2*). The same was true for **9** with MIC = 8 μM, which was designed for Cys-Lys stapling in aprotic media,[30] but presumably hydrolyzed to the carboxylate before reacting at the cell surface (*Figure 2*).

The most active hypervalent iodine reagents with MIC ≤ 2 μM showed less than perfect dose response curves. Ethynyl benziodoxolone **2** suffered from a rather early onset of toxicity, exceeding activity above the IC_{50} = 10 μM (*Figure 4,e*). Azide **4** showed an intriguing, almost concentration independent inhibition around 30% from MIC ≤ 2 μM until the onset of toxicity >50 μM (*Figure 4,f*). As already mentioned, competing precipitation or the onset of toxicity related activation could contribute to this apparent concentration independence. Moreover, the environment-dependent contributions from the addition of exofacial thiols **27** to yield alkene **28** rather than the standard substitution product **29** could contribute to unusual dose response (*Figure 5*).[28] The same behav-

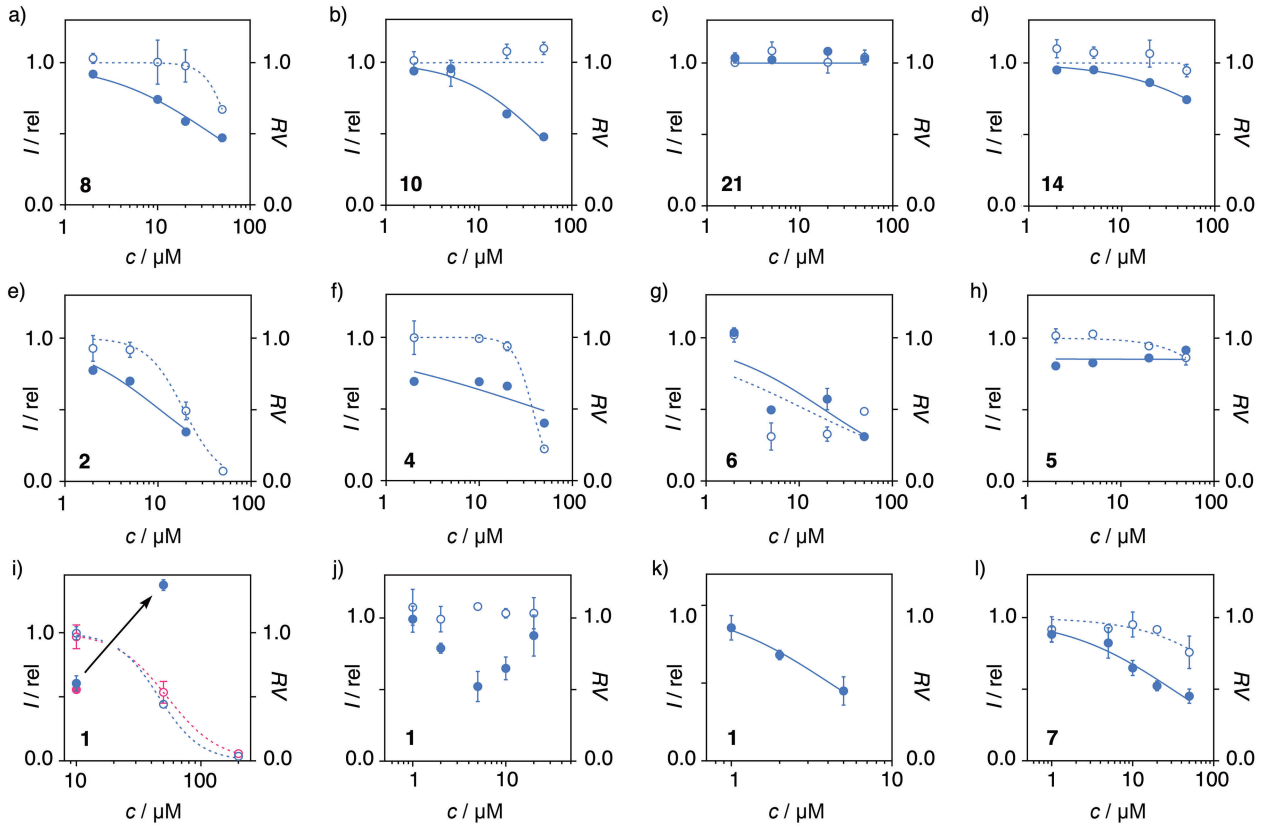

Figure 4. Representative HCHTS profiles showing relative fluorescence intensity *I* (filled symbols) and relative cell viability *RV* (empty symbols) of HeLa Kyoto cells after incubation with a) **8**, b) **10**, c) **21**, d) **14**, e) **2**, f) **4**, g) **6**, h) **5**, i–k) **1** and l) **7** for 1 h at the indicated concentrations, followed by incubation with the fluorescent reporter **26** (10 µM) for 30 min. i–k) Screening optimization for **1**: i) Initial tests revealing the onset of toxicity (empty symbols) and toxicity related activation (arrow) between 10 and 50 µM; blue: 1 h, pink: 30 min incubation with **26**; j) focused tests at lower concentrations, demonstrating the onset of toxicity related activation between 5 and 10 µM; k) curve fit for inhibition until onset of activation above 5 µM, revealing MIC and IC_{50}.

ior at weaker inhibition of *ca.* 15% was observed with **5** (*Figure 4,h*), while **6** was simply too toxic to be considered (*Figure 4,g*). More convincing dose response curves appeared with **8** at MIC = 4 µM (*Figure 4,a*). The less reactive amidines generally excelled with low toxicity also at high concentrations. The dose response curves for **10** with an MIC = 8 µM could be completed below a high IC_{50} = 42 µM without the appearance of toxicity (*Figure 4,b*).

Irreversible inhibition of thiol-mediated uptake with hypervalent iodine reagents compared favorably to other reagents. Tunable heteroaromatic sulfones like **16** have been introduced recently as bioorthogonal probes for cysteine profiling.[37] They react with thiols by nucleophilic aromatic substitution, affording aryl sulfides **30** (*Figure 5*). As reported previously,[20] inhibition of thiol-mediated uptake with heteroaromatic sulfones nicely follows reactivity from **24** with MIC = 300 µM over **17** with MIC = 40 µM to **16** with MIC = 15 µM, but overall activities were not competitive (*Figure 2*). The same was true for the related, electron-deficient 2-sulfonylpyridines **22** and **23** introduced by *Zambaldo et al.* for the targeted labeling of proteins with stable aryl sulfides **31** (*Figure 5*).[38] Activities increased from **23** to **22**, but the best MIC = 100 µM was not impressive, only five times better than *Ellman*'s reagent (*Figure 2*).

The 3-arylpropiolonitrile **13** introduced by *Wagner* and coworkers[36] for ultrafast, bioorthogonal and irreversible conjugate 'click' addition of cysteines to afford conjugates **32** gave better results, with an MIC = 19 µM and an onset of competing activation visible above 50 µM (*Figures 2* and *5*). The most positive surprise, however, was DNs protected glutamate **7**. A classic in organic synthesis, nosyl deprotection occurs also by nucleophilic aromatic substitution with thiols **27** to afford sulfide **33** besides the deprotected amine and SO_2 (*Figure 5*).[34] Inhibition of thiol-mediated

uptake of reporter **26** by DNs **7** occurred with an MIC = 2.1 μM, an IC_{50} = 31 μM and a dose response curve without significant anomalies (*Figures 2* and *4,l*).

Among the best inhibitors were super-cinnamaldehydes **1** and **3**. These activated *Michael* acceptors were introduced by *Cravatt*, *Schultz* and coworkers to elucidate the mode of action of TRPA1 (transient receptor potential ankyrin 1).[35] TRPA1 is an ion channel that is activated by pain, cold and itch, responding to noxious stimuli from pungent natural products such as cinnamaldehyde, mustard oil, or allicin from garlic.[35,58] Super-cinnamaldehydes **1** and **3** were rationally designed to explore whether or not the ion channel is activated by conjugate addition of thiols. Their activity was found to exceed cinnamaldehyde, thus validating the hypothesis of covalent ion channel activation. Conjugate addition to yield sulfide **34** was shown to be irreversible (*Figure 5*).[35] Molecular recognition by TRPA1 is likely to direct the regioselectivity of the *Michael* addition to mimic cinnamaldehyde as drawn in **34**, whereas intrinsic reactivity in solution should favor addition to the exocyclic carbon.[59]

The inhibition of thiol-mediated uptake of reporter **26** by super-cinnamaldehydes was slightly better for the more hydrophobic **1** than for **3** (*Figure 2*). Both *Michael* acceptors gave anomalous dose response curves in initial screens, with promising inhibition around 10 μM changing to significant activation and high toxicity at 50 μM (*Figure 4,i*). Focused screening around 10 μM gave a sub-micromolar MIC < 1 μM and a minimum around the IC_{50} = 4 μM, followed by decreasing inhibition at higher concentrations due to increasingly dominant uptake activation (*Figure 4,j*). Remarkably, this IC_{50} = 4 μM of super-cinnamaldehyde **1** was below the best hypervalent iodine reagent **2** with IC_{50} = 10 μM and not affected by cytotoxicity at this relevant concentration (*Figures 2* and *4,i*).

It would be premature to conclude that TRPA1 can contribute to thiol-mediated uptake. The cysteines

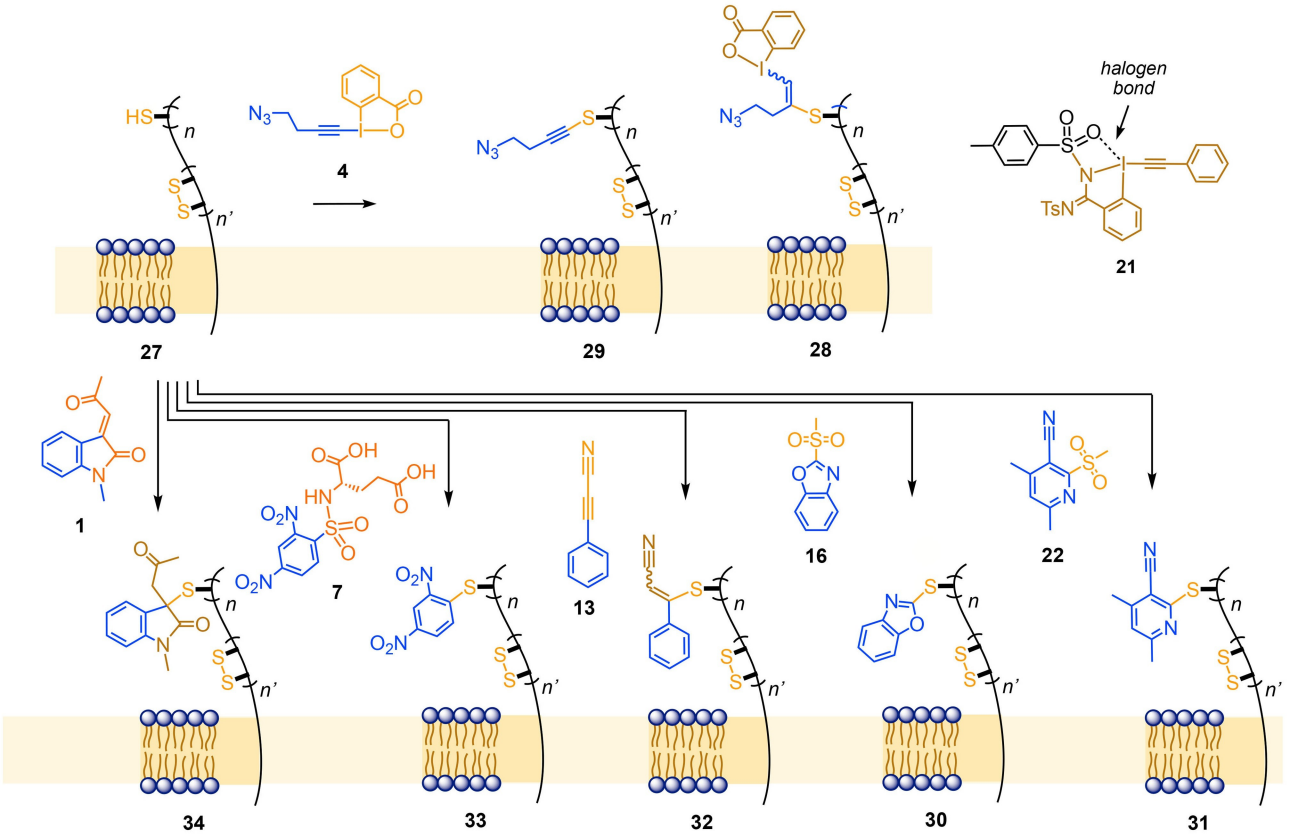

Figure 5. Irreversible reactions of hypervalent iodine reagents compared to other key motifs with thiols on cell surfaces. Substitution products like **29** are generally preferred, addition products like **28** occur with alkyl alkynes, depending on the environment. An intramolecular halogen bond is thought to account for reduced reactivity of **21** and related inhibitors.

targeted by super-cinnamaldehyde **1** are on the luminal side of the ion channel and not accessible by larger substrates. However, TRPA1 contains cysteines within transmembrane helices that could conceivably be involved in thiol-mediated uptake as outlined elsewhere.[1] More likely, however, is that super-cinnamaldehydes **1** and **3** react with other, so far unknown targets on the cell surface with exofacial thiols that mediate cellular uptake.

In summary, screening of the so far largest collection of hypervalent iodine reagents to inhibit thiol-mediated uptake of a fluorescent ETP reporter afforded activities that, with MIC < 2 μM, rival the best COCs identified so far and exceed the activity of the benchmark DTNB more than 250 times. Inhibition overall correlated well with reactivity. Anomalous dose response curves could be rationalized with the onset of activation by membrane destabilization and, perhaps, aggregation and precipitation. Activities compare well with other irreversible thiol-reactive agents, which increase with reactivity within a given class but vary strongly between different classes. These reactivity-independent variations demonstrate that thiol-mediated uptake operates with important selectivity, that is molecular recognition. Similarly significant contributions from molecular recognition have been observed in proteomics studies with the same and similar thiol-reactive probes. Each probe labeled different protein families in the cysteinome.[27,37,44] Thiol-mediated uptake thus emerges as functional system to elucidate parts of the cysteinome 'in action'.

The distinct signatures of irreversible inhibitors further confirm that thiol-mediated uptake exists and involves significant molecular recognition. Simple passive diffusion also of small-molecule reporters like **26** across the plasma membrane can thus be excluded. Together with hypervalent iodine reagents, nosyl protecting groups and super-cinnamaldehydes emerge as unexpected and most promising scaffolds to further elaborate on irreversible inhibitors of thiol-mediated uptake and beyond.

Acknowledgements

We thank the NMR and MS platforms for service, and the University of Geneva, including an Innogap Grant (S.M.), the Swiss National Centre of Competence in Research (NCCR) Chemical Biology (J.W., S.M.), the NCCR Molecular Systems Engineering (S.M.), the Swiss NSF (200020 182798 (J.W.), 200020 175486 (S.M.)) and the European Research Council (ERC Consolidator Grant SeleCHEM No. 771170, J.W.) for financial support.

Author Contributions Statement

B. L., *Y. C.* and *D. M.* performed the inhibitor screening, *T. K.*, *A.-T. P.*, *E. L. D.*, *A. K. M.* and *E. G.* synthesized inhibitors, *N. S.*, *J. W.* and *S. M.* directed the study, all authors contributed to experimental design, data interpretation and manuscript writing.

References

[1] Q. Laurent, R. Martinent, B. Lim, A.-T. Pham, T. Kato, J. López-Andarias, N. Sakai, S. Matile, 'Thiol-Mediated Uptake', *JACS Au* **2021**, *1*, 710–728.
[2] A. Tirla, P. Rivera-Fuentes, 'Peptide Targeting of an Intracellular Receptor of the Secretory Pathway', *Biochemistry* **2019**, *58*, 1184–1187.
[3] A. F. L. Schneider, M. Kithil, M. C. Cardoso, M. Lehmann, C. P. R. Hackenberger, 'Cellular uptake of large biomolecules enabled by cell-surface-reactive cell-penetrating peptide additives', *Nat. Chem.* **2021**, *13*, 530–539.
[4] S. Du, S. S. Liew, L. Li, S. Q. Yao, 'Bypassing Endocytosis: Direct Cytosolic Delivery of Proteins', *J. Am. Chem. Soc.* **2018**, *140*, 15986–15996.
[5] A. G. Torres, M. J. Gait, 'Exploiting cell surface thiols to enhance cellular uptake', *Trends Biotechnol.* **2012**, *30*, 185–190.
[6] S. Ulrich, 'Growing Prospects of Dynamic Covalent Chemistry in Delivery Applications', *Acc. Chem. Res.* **2019**, *52*, 510–519.
[7] J. Zhou, Z. Shao, J. Liu, Q. Duan, X. Wang, J. Li, H. Yang, 'From Endocytosis to Nonendocytosis: The Emerging Era of Gene Delivery', *ACS Appl. Bio Mater.* **2020**, *3*, 2686–2701.
[8] X. Meng, T. Li, Y. Zhao, C. Wu, 'CXC-Mediated Cellular Uptake of Miniproteins: Forsaking "Arginine Magic"', *ACS Chem. Biol.* **2018**, *13*, 3078–3086.
[9] J. Lu, H. Wang, Z. Tian, Y. Hou, H. Lu, 'Cryopolymerization of 1,2-Dithiolanes for the Facile and Reversible Grafting-from Synthesis of Protein-Polydisulfide Conjugates', *J. Am. Chem. Soc.* **2020**, *142*, 1217–1221.
[10] J. Zhou, L. Sun, L. Wang, Y. Liu, J. Li, J. Li, J. Li, H. Yang, 'Self-Assembled and Size-Controllable Oligonucleotide Nanospheres for Effective Antisense Gene Delivery through an Endocytosis-Independent Pathway', *Angew. Chem. Int. Ed.* **2019**, *58*, 5236–5240.
[11] D. Oupický, J. Li, 'Bioreducible Polycations in Nucleic Acid Delivery: Past, Present, and Future Trends', *Macromol. Biosci.* **2014**, *14*, 908–922.
[12] Z. Shu, I. Tanaka, A. Ota, D. Fushihara, N. Abe, S. Kawaguchi, K. Nakamoto, F. Tomoike, S. Tada, Y. Ito, Y. Kimura, H. Abe, 'Disulfide-Unit Conjugation Enables Ultrafast Cytosolic Internalization of Antisense DNA and siRNA', *Angew. Chem. Int. Ed.* **2019**, *58*, 6611–6615.

[13] A. Kohata, P. K. Hashim, K. Okuro, T. Aida, 'Transferrin-Appended Nanocaplet for Transcellular siRNA Delivery into Deep Tissues', *J. Am. Chem. Soc.* **2019**, *141*, 2862–2866.
[14] Q. Laurent, N. Sakai, S. Matile, 'The Opening of 1,2-Dithiolanes and 1,2-Diselenolanes: Regioselectivity, Rearrangements, and Consequences for Poly(disulfide)s, Cellular Uptake and Pyruvate Dehydrogenase Complexes', *Helv. Chim. Acta* **2019**, *102*, e1800209.
[15] H. J.-P. Ryser, R. Flückiger, 'Keynote review: Progress in targeting HIV-1 entry', *Drug Discovery Today* **2005**, *10*, 1085–1094.
[16] G. Gasparini, G. Sargsyan, E.-K. Bang, N. Sakai, S. Matile, 'Ring Tension Applied to Thiol-Mediated Cellular Uptake', *Angew. Chem. Int. Ed.* **2015**, *54*, 7328–7331.
[17] Y. Okamoto, R. Kojima, F. Schwizer, E. Bartolami, T. Heinisch, S. Matile, M. Fussenegger, T. R. Ward, 'A cell-penetrating artificial metalloenzyme regulates a gene switch in a designer mammalian cell', *Nat. Commun.* **2018**, *9*, 1943.
[18] E. Derivery, E. Bartolami, S. Matile, M. Gonzalez-Gaitan, 'Efficient Delivery of Quantum Dots into the Cytosol of Cells Using Cell-Penetrating Poly(disulfide)s', *J. Am. Chem. Soc.* **2017**, *139*, 10172–10175.
[19] N. Chuard, G. Gasparini, D. Moreau, S. Lörcher, C. Palivan, W. Meier, N. Sakai, S. Matile, 'Strain-Promoted Thiol-Mediated Cellular Uptake of Giant Substrates: Liposomes and Polymersomes', *Angew. Chem. Int. Ed.* **2017**, *56*, 2947–2950.
[20] Y. Cheng, A.-T. Pham, T. Kato, B. Lim, D. Moreau, J. López-Andarias, L. Zong, N. Sakai, S. Matile, 'Inhibitors of thiol-mediated uptake', *Chem. Sci.* **2021**, *12*, 626–631.
[21] K. Sargsyan, C.-C. Lin, T. Chen, C. Grauffel, Y.-P. Chen, W.-Z. Yang, H. S. Yuan, C. Lim, 'Multi-targeting of functional cysteines in multiple conserved SARS-CoV-2 domains by clinically safe Zn-ejectors', *Chem. Sci.* **2020**, *11*, 9904–9909.
[22] Z. Jin, X. Du, Y. Xu, Y. Deng, M. Liu, Y. Zhao, B. Zhang, X. Li, L. Zhang, C. Peng, Y. Duan, J. Yu, L. Wang, K. Yang, F. Liu, R. Jiang, X. Yang, T. You, X. Liu, X. Yang, F. Bai, H. Liu, X. Liu, L. W. Guddat, W. Xu, G. Xiao, C. Qin, Z. Shi, H. Jiang, Z. Rao, H. Yang, 'Structure of M^{pro} from SARS-CoV-2 and discovery of its inhibitors', *Nature* **2020**, *582*, 289–293.
[23] D. Abegg, G. Gasparini, D. G. Hoch, A. Shuster, E. Bartolami, S. Matile, A. Adibekian, 'Strained Cyclic Disulfides Enable Cellular Uptake by Reacting with the Transferrin Receptor', *J. Am. Chem. Soc.* **2017**, *139*, 231–238.
[24] X. Tang, M. Yang, Z. Duan, Z. Liao, L. Liu, R. Cheng, M. Fang, G. Wang, H. Liu, J. Xu, P. M. Kamau, Z. Zhang, L. Yang, X. Zhao, X. Peng, R. Lai, 'Transferrin receptor is another receptor for SARS-CoV-2 entry', *bioRxiv* **2020**, doi.org/10.1101/2020.10.23.350348.
[25] R. Frei, J. Waser, 'A Highly Chemoselective and Practical Alkynylation of Thiols', *J. Am. Chem. Soc.* **2013**, *135*, 9620–9623.
[26] R. Frei, M. D. Wodrich, D. P. Hari, P.-A. Borin, C. Chauvier, J. Waser, 'Fast and Highly Chemoselective Alkynylation of Thiols with Hypervalent Iodine Reagents Enabled through a Low Energy Barrier Concerted Mechanism', *J. Am. Chem. Soc.* **2014**, *136*, 16563–16573.
[27] D. Abegg, R. Frei, L. Cerato, D. P. Hari, C. Wang, J. Waser, A. Adibekian, 'Proteome-Wide Profiling of Targets of Cysteine reactive Small Molecules by Using Ethynyl Benziodoxolone Reagents', *Angew. Chem. Int. Ed.* **2015**, *54*, 10852–10857.
[28] R. Tessier, J. Ceballos, N. Guidotti, R. Simonet-Davin, B. Fierz, J. Waser, '"Doubly Orthogonal" Labeling of Peptides and Proteins', *Chem* **2019**, *5*, 2243–2263.
[29] R. Tessier, R. K. Nandi, B. G. Dwyer, D. Abegg, C. Sornay, J. Ceballos, S. Erb, S. Cianférani, A. Wagner, G. Chaubet, A. Adibekian, J. Waser, 'Ethynylation of Cysteine Residues: From Peptides to Proteins in Vitro and in Living Cells', *Angew. Chem. Int. Ed.* **2020**, *59*, 10961–10970.
[30] J. Ceballos, E. Grinhagena, G. Sangouard, C. Heinis, J. Waser, 'Cys-Cys and Cys-Lys Stapling of Unprotected Peptides Enabled by Hypervalent Iodine Reagents', *Angew. Chem. Int. Ed.* **2021**, *60*, 9022–9031.
[31] P. Morelli, X. Martin-Benlloch, R. Tessier, J. Waser, N. Sakai, S. Matile, 'Ethynyl benziodoxolones: functional terminators for cell-penetrating poly(disulfide)s', *Polym. Chem.* **2016**, *7*, 3465–3470.
[32] Y. Li, D. P. Hari, M. V. Vita, J. Waser, 'Cyclic Hypervalent Iodine Reagents for Atom-Transfer Reactions: Beyond Trifluoromethylation', *Angew. Chem. Int. Ed.* **2016**, *55*, 4436–4454.
[33] D. P. Hari, P. Caramenti, J. Waser, 'Cyclic Hypervalent Iodine Reagents: Enabling Tools for Bond Disconnection via Reactivity Umpolung', *Acc. Chem. Res.* **2018**, *51*, 3212–3225.
[34] T. Kan, T. Fukuyama, 'Ns strategies: a highly versatile synthetic method for amines', *Chem. Commun.* **2004**, 353–359.
[35] L. J. Macpherson, A. E. Dubin, M. J. Evans, F. Marr, P. G. Schultz, B. F. Cravatt, A. Patapoutian, 'Noxious compounds activate TRPA1 ion channels through covalent modification of cysteines', *Nature* **2007**, *445*, 541–545.
[36] O. Koniev, G. Leriche, M. Nothisen, J.-S. Remy, J.-M. Strub, C. Schaeffer-Reiss, A. Van Dorsselaer, R. Baati, A. Wagner, 'Selective Irreversible Chemical Tagging of Cysteine with 3-Arylpropiolonitriles', *Bioconjugate Chem.* **2014**, *25*, 202–206.
[37] H. F. Motiwala, Y.-H. Kuo, B. L. Stinger, B. A. Palfey, B. R. Martin, 'Tunable Heteroaromatic Sulfones Enhance in-Cell Cysteine Profiling', *J. Am. Chem. Soc.* **2020**, *142*, 1801–1810.
[38] C. Zambaldo, E. V. Vinogradova, X. Qi, J. Iaconelli, R. M. Suciu, M. Koh, K. Senkane, S. R. Chadwick, B. B. Sanchez, J. S. Chen, A. K. Chatterjee, P. Liu, P. G. Schultz, B. F. Cravatt, M. J. Bollong, '2-Sulfonylpyridines as Tunable, Cysteine-Reactive Electrophiles', *J. Am. Chem. Soc.* **2020**, *142*, 8972–8979.
[39] Y.-C. Ahn, V. K. May, G. C. Bedford, A. A. Tuley, W. Fast, 'Discovery of 4,4′-Dipyridylsulfide Analogs as "Switchable Electrophiles" for Covalent Inhibition', *ACS Chem. Biol.* **2021**, *16*, 264–269.
[40] Q. Liu, Y. Sabnis, Z. Zhao, T. Zhang, S. J. Buhrlage, L. H. Jones, N. S. Gray, 'Developing Irreversible Inhibitors of the Protein Kinase Cysteinome', *Chem. Biol.* **2013**, *20*, 146–159.
[41] F. S. Steven, V. Podrazký, 'Evidence for the Inhibition of Trypsin by Thiols', *Eur. J. Biochem.* **1978**, *83*, 155–161.
[42] M. E. B. Smith, F. F. Schumacher, C. P. Ryan, L. M. Tedaldi, D. Papaioannou, G. Waksman, S. Caddick, J. R. Baker, 'Protein Modification, Bioconjugation, and Disulfide Bridging Using

Bromomaleimides', *J. Am. Chem. Soc.* **2010**, *132*, 1960–1965.
[43] A. J. Rojas, C. Zhang, E. V. Vinogradova, N. H. Buchwald, J. Reilly, B. L. Pentelute, S. L. Buchwald, 'Divergent unprotected peptide macrocyclisation by palladium-mediated cysteine arylation', *Chem. Sci.* **2017**, *8*, 4257–4263.
[44] K. Tokunaga, M. Sato, K. Kuwata, C. Miura, H. Fuchida, N. Matsunaga, S. Koyanagi, S. Ohdo, N. Shindo, A. Ojida, 'Bicyclobutane Carboxylic Amide as a Cysteine-Directed Strained Electrophile for Selective Targeting of Proteins', *J. Am. Chem. Soc.* **2020**, *142*, 18522–18531.
[45] A.-T. Pham, S. Matile, 'Peptide Stapling with Anion-π Catalysts', *Chem. Asian J.* **2020**, *15*, 1562–1566.
[46] L. Zong, E. Bartolami, D. Abegg, A. Adibekian, N. Sakai, S. Matile, 'Epidithiodiketopiperazines: Strain-Promoted Thiol-Mediated Cellular Uptake at the Highest Tension', *ACS Cent. Sci.* **2017**, *3*, 449–453.
[47] R. Martinent, J. López-Andarias, D. Moreau, Y. Cheng, N. Sakai, S. Matile, 'Automated high-content imaging for cellular uptake, from the Schmuck cation to the latest cyclic oligochalcogenides', *Beilstein J. Org. Chem.* **2020**, *16*, 2007–2016.
[48] E. Le Du, T. Duhail, M. D. Wodrich, R. Scopelliti, F. Fadaei-Tirani, E. Anselmi, E. Magnier, J. Waser, 'Structure and Reactivity of *N*-Heterocyclic Alkynyl Hypervalent Iodine Reagents', *Chem. Eur. J.* **2021**, doi.org/10.1002/chem.202101475.
[49] G. Cavallo, P. Metrangolo, R. Milani, T. Pilati, A. Priimagi, G. Resnati, G. Terraneo, 'The Halogen Bond', *Chem. Rev.* **2016**, *116*, 2478–2601.
[50] M. S. Taylor, 'Anion recognition based on halogen, chalcogen, pnictogen and tetrel bonding', *Coord. Chem. Rev.* **2020**, *413*, 213270.
[51] L. E. Bickerton, A. J. Sterling, P. D. Beer, F. Duarte, M. J. Langton, 'Transmembrane anion transport mediated by halogen bonding and hydrogen bonding triazole anionophores', *Chem. Sci.* **2020**, *11*, 4722–4729.
[52] R. L. Sutar, S. M. Huber, 'Catalysis of Organic Reactions through Halogen Bonding', *ACS Catal.* **2019**, *9*, 9622–9639.
[53] K. Strakova, L. Assies, A. Goujon, F. Piazzolla, H. V. Humeniuk, S. Matile, 'Dithienothiophenes at Work: Access to Mechanosensitive Fluorescent Probes, Chalcogen-Bonding Catalysis, and Beyond', *Chem. Rev.* **2019**, *119*, 10977–11005.
[54] A. Gini, M. Paraja, B. Galmés, C. Besnard, A. I. Poblador-Bahamonde, N. Sakai, A. Frontera, S. Matile, 'Pnictogen-bonding catalysis: brevetoxin-type polyether cyclizations', *Chem. Sci.* **2020**, *11*, 7086–7091.
[55] J. García-Calvo, J. Maillard, I. Fureraj, K. Strakova, A. Colom, V. Mercier, A. Roux, E. Vauthey, N. Sakai, A. Fürstenberg, S. Matile, 'Fluorescent Membrane Tension Probes for Super-Resolution Microscopy: Combining Mechanosensitive Cascade Switching with Dynamic-Covalent Ketone Chemistry', *J. Am. Chem. Soc.* **2020**, *142*, 12034–12038.
[56] N. Declas, G. Pisella, J. Waser, 'Vinylbenziodoxol(on)es: Synthetic Methods and Applications', *Helv. Chim. Acta* **2020**, *103*, e2000191.
[57] A. K. Mishra, R. Tessier, D. P. Hari, J. Waser, 'Amphiphilic Iodine(III) Reagents for the Lipophilization of Peptides in Water', *Angew. Chem. Int. Ed.* **2021**, doi.org/10.1002/anie.202106458.
[58] D. M. Bautista, P. Movahed, A. Hinman, H. E. Axelsson, O. Sterner, E. D. Högestätt, D. Julius, S.-E. Jordt, P. M. Zygmunt, 'Pungent products from garlic activate the sensory ion channel TRPA1', *Proc. Natl. Acad. Sci. USA* **2005**, *102*, 12248–12252.
[59] J. Sun, Y.-J. Xie, C.-G. Yan, 'Construction of Dispirocyclopentanebisoxindoles via Self-Domino Michael-Aldol Reactions of 3-Phenacylideneoxindoles', *J. Org. Chem.* **2013**, *78*, 8354–8365.

Received June 1, 2021
Accepted June 23, 2021

HELVETICA
chimica acta

Supporting Information

Inhibition of Thiol-Mediated Uptake with Irreversible Covalent Inhibitors

Bumhee Lim[+], Yangyang Cheng[+], Takehiro Kato[+], Anh-Tuan Pham, Eliott Le Du, Abhaya Kumar Mishra, Elija Grinhagena, Dimitri Moreau, Naomi Sakai, Jerome Waser,* and Stefan Matile*

Supporting Information

Inhibition of Thiol-Mediated Uptake with Irreversible Covalent Inhibitors

Bumhee Lim, Yangyang Cheng, Takehiro Kato, Anh-Tuan Pham, Eliott Le Du,

Abhaya Kumar Mishra, Elija Grinhagena, Dimitri Moreau, Naomi Sakai,

Jerome Waser* and Stefan Matile*

Department of Organic Chemistry, University of Geneva, Switzerland,

Laboratory of Catalysis and Organic Synthesis, Ecole Polytechnique Fédérale de Lausanne

EPFL SB ISIC LCSO, Switzerland

jerome.waser@epfl.ch; stefan.matile@unige.ch

Table of Contents

1. General Methods

All reactions that were carried out in oven dried glassware and under an atmosphere of nitrogen is stated at the start of the reaction conditions. For flash chromatography, distilled technical grade solvents were used. THF, CH_3CN, toluene, Et_2O and CH_2Cl_2 were dried by passage over activated alumina under nitrogen atmosphere (H_2O content < 10 ppm, Karl-Fischer titration). The solvents were degassed by Freeze-Pump-Thaw method when mentioned. All chemicals were purchased from Acros, Aldrich, Fluka, VWR, TCI, Merck and used as such unless stated otherwise. Chromatographic purification was performed as flash chromatography using Macherey-Nagel silica 40-63, 60 Å, using the solvents indicated as eluent with 0.1-0.5 bar pressure. TLC was performed on Merck silica gel 60 F254 TLC glass plates and visualized with UV light and *p*-anisaldehyde stain (EtOH:H_2SO_4:AcOH:*p*-anisaldehyde 135:5:1.5:3.7 V:V:V:V).

^{1}H-NMR spectra were recorded on a Bruker DPX-400 400 MHz spectrometer in $CDCl_3$, CD_3CN, CD_3OD, DMSO-d_6 or acetone-d_6, all signals are reported in ppm with the internal chloroform signal at 7.26 ppm, the internal acetonitrile signal at 1.94 ppm, the internal methanol signal at 3.30 ppm, the internal DMSO signal at 2.50 ppm or the internal acetone signal at 2.05 ppm as standard. The data is reported as (s = singlet, d = doublet, t= triplet, q = quadruplet, qi = quintet, m = multiplet or unresolved, br = broad signal, app = apparent, coupling constant(s) in Hz, integration, interpretation). ^{13}C-NMR spectra were recorded with ^{1}H-decoupling on a Bruker DPX-400 100 MHz spectrometer in $CDCl_3$, CD_3CN, CD_3OD, DMSO-d_6 or acetone-d_6, all signals are reported in ppm with the internal chloroform signal at 77.0 ppm, the internal acetonitrile signal at 1.3 ppm, the internal methanol signal at 49.0 ppm, the internal DMSO signal at 39.5 ppm or the internal acetone signals at 29.84 and 206.26 ppm as standard. Rotameric mixtures have been described at rt as a mixture of rotamers, only the split signals have been assigned to the major or minor rotamer. Regiomeric mixtures have been assigned

based on the shift of the characteristic proton signals. Diastereoiomers have been separated when possible if not assigned based on ^{1}H NMR analysis. Infrared spectra were recorded on a JASCO FT-IR B4100 spectrophotometer with an ATR PRO410-S and a ZnSe prisma or Perkin Elmer Spectrum 100 FT-IR spectrometer (ATR, Golden Gate, unless stated) and is reported in cm^{-1} (w = weak, m = medium, s = strong, br = broad). High resolution mass spectrometric measurements were performed by the mass spectrometry service of ISIC at the EPFL on a MICROMASS (ESI) Q-TOF Ultima API.

Abbreviations. Ac_2O: Acetic anhydride; aq.: aqueous; COCs: Cyclic oligochalcogenides; DCE: 1,2-Dichloroethane; DIPEA: *N,N*-Diisopropylethylamine; DMAP: 4-dimethylaminopyridine; DMEM: Dulbecco's modified eagle medium; DMF: *N*,*N*-Dimethylformamide; DMSO: Dimethyl sulfoxide; DNs: Dinitrobenzenesulfonyl; DTNB: 5,5-dithio-bis(2-nitrobenzoic acid); EBX: Ethynyl benziodoxolone; EtOAc: Ethyl acetate; ETP: Epidithiodiketopiperazine; FITC: fluorescein; GI_{50}: Half maximal cell growth inhibition concentration; HCHT: High-content high-throughput; IC_{50}: Half maximal inhibitory concentration; LiHMDS: Lithium bis(trimethylsilyl)amide; *m*CPBA: *meta*-chloroperoxybenzoic acid; MICs: Minimum inhibitory concentrations; MTS: 3-(4,5-Dimethylthiazol-2-yl)-5-(3-carboxymethoxyphenyl)-2-(4-sulfophenyl)-2*H*-tetrazolium; PBS: Phosphate buffer saline; *p*-TsOH·H_2O: *para*-toluene sulfonic acid monohydrate; rt: room temperature; PI: Propidium iodide; RV: Relative viability; sat.: saturated; Tf: Trifluoromethanesulfonyl; TFA: Trifluoroacetic acid; TFE: 2,2,2-Trifluoroethanol; THF: Tetrahydrofuran; TIPS: Triisopropylsilyl; TMS: Trimethylsilyl; Ts: 4-Toluenesulfonyl.

2. Synthesis

2.1. Synthesis of Reporter

Fluorescein-epidithiodiketopiperazine (FITC-ETP, **26**) was synthesized and purified according to procedures described in reference [S1].

2.2. Synthesis of Hypervalent Iodine Reagents

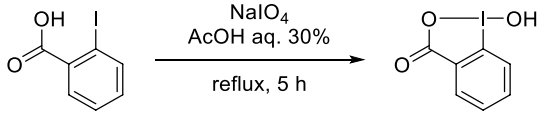

35 **36**

1-Hydroxy-1,2-benziodoxol-3-(1*H*)-one (36). Following a reported procedure,[S2] $NaIO_4$ (40.5 g, 189 mmol, 1.05 equiv) and 2-iodobenzoic acid (**35**) (44.8 g, 180 mmol, 1.0 equiv) were suspended in 30% (v:v) aq. AcOH (350 mL). The mixture was vigorously stirred and refluxed for 5 h. The reaction mixture was then diluted with cold water (250 mL) and allowed to cool to rt, protecting it from light. After 1 h, the crude product was collected by filtration, washed on the filter with ice water (3 × 150 mL) and acetone (3 × 150 mL), and air-dried in the dark overnight to afford 1-hydroxy-1,2-benziodoxol-3-(1*H*)-one (**36**) (44.3 g, 168 mmol, 93% yield) as a white solid. ^{1}H NMR (400 MHz, DMSO-d_6) δ 8.02 (dd, J = 7.7, 1.4 Hz, 1H, Ar*H*), 7.97 (m, 1H, Ar*H*), 7.85 (dd, J = 8.2, 0.7 Hz, 1H, Ar*H*), 7.71 (td, J = 7.6, 1.2 Hz, 1H, Ar*H*); ^{13}C NMR (100 MHz, DMSO-d_6) δ 167.7, 134.5, 131.5, 131.1, 130.4, 126.3, 120.4. Consistent with reported data.[S2]

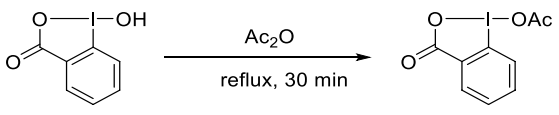

36 **37**

1-Acetoxy-1,2-benziodoxol-3-(1*H*)-one (37). Following a reported procedure,[S3] compound **36** (3.00 g, 11.3 mmol, 1.00 equiv) was heated in Ac_2O (10 mL) to reflux until the

solution turned clear (without suspension, ca. 30 min). The mixture was then left to cool down and white crystals started to form. The crystallization was continued at -18 °C. The crystals were then collected and dried overnight under high vacuum to give compound **37** (3.06 g, 10.0 mmol, 86% yield). ^{1}H NMR (400 MHz, $CDCl_3$) δ 8.25 (dd, 1 H, *J* = 7.6, 1.4 Hz, Ar*H*), 8.00 (dd, 1 H, *J* = 8.3, 0.5 Hz, Ar*H*), 7.92 (dt, 1 H, *J* = 7.0, 1.7 Hz, Ar*H*), 7.71 (td, 1 H, *J* = 7.6, 0.9 Hz, Ar*H*), 2.25 (s, 3 H, COC*H*$_3$). NMR data correspond to the reported values.[S3]

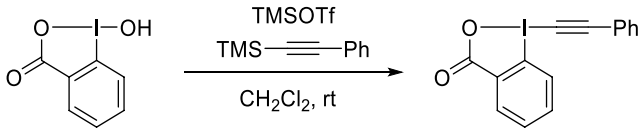

36 **2**

1-[Phenylethynyl]-1,2-benziodoxol-3(1*H*)-one (Ph-EBX, 2). Following a reported procedure,[S4] trimethylsilyltriflate (9.1 mL, 50 mmol, 1.1 equiv) was added dropwise to a suspension of 2-iodosylbenzoic acid (**36**) (12.1 g, 45.8 mmol, 1.0 equiv) in CH_2Cl_2 (120 mL) at 0 °C. The mixture was stirred for 1 h, followed by the dropwise addition of trimethyl-(phenylethynyl)silane (8.8 mL, 50 mmol, 1.1 equiv) (slightly exothermic). The resulting suspension was stirred for 6 h at rt, during this time a white solid was formed. sat. $NaHCO_3$ aq. (120 mL) was added and the mixture was stirred vigorously for 30 min. The resulting suspension was filtered on a glass filter. The two layers of the mother liquor were separated and the organic layer was washed with sat. $NaHCO_3$ aq. (2 × 50 mL), dried over $MgSO_4$, filtered and evaporated under reduced pressure. The resulting mixture was combined with the solid obtained by recrystallisation in EtOAc/MeOH (2:1, ca. 28 mL/g). The mixture was cooled down, filtered and dried under high vacuum to afford Ph-EBX (**2**) (6.8 g, 25 mmol, 43% yield) as colorless crystals. Mp (Dec.) 155–160 °C; ^{1}H NMR (400 MHz, $CDCl_3$) δ 8.46 (m, 1H, ArH), 8.28 (m, 1H, ArH), 7.80 (m, 2H, ArH), 7.63 (m, 2H, ArH), 7.48 (m, 3H, ArH); ^{13}C NMR (101

MHz, $CDCl_3$) δ 163.9, 134.9, 132.9, 132.5, 131.6, 131.3. 130.8, 128.8, 126.2, 120.5, 116.2, 106.6, 50.2. Consistent with reported data.[S2]

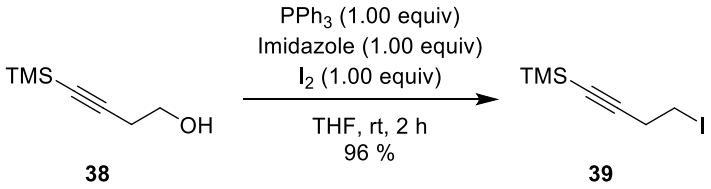

(4-Iodo-but-1-yn-1-yl)trimethylsilane (39). Following a slightly modified procedure,[S5] triphenylphosphine (PPh_3, 37.9 g, 145 mmol, 1.00 equiv) was added to a cooled solution of 4-(trimethylsilyl)but-3-yn-1-ol (**38**) (20.6 g, 145 mmol, 1.00 equiv) in THF (545 mL) at 0 °C. Upon dissolution, imidazole (9.84 g, 145 mmol, 1.00 equiv) was added, followed by iodine (I_2, 36.7 g, 145 mmol, 1.00 equiv). The resulting mixture was then allowed to warm to rt and was stirred for 2 h. It was then diluted with Et_2O (400 mL) and washed with 10% aqueous sodium thiosulfate (400 mL). The aqueous layer was extracted with additional portions of Et_2O (2 × 150 mL) and the combined organic layers were washed with brine (400 mL), dried over $MgSO_4$, filtered and concentrated *in vacuo*. The resulting white suspension was filtered through a plug of silica, eluting with pentane, to afford pure (4-iodo-but-1-yn-1-yl)trimethylsilane (**39**) (34.9 g, 138 mmol, 96% yield) as a colorless oil. ^{1}H NMR (400 MHz, $CDCl_3$) δ 3.20 (t, J = 7.5 Hz, 2H, CH_2CH_2I), 2.78 (t, J = 7.5 Hz, 2H, CH_2CH_2I), 0.14 (s, 9H, TMS); ^{13}C NMR (101 MHz, $CDCl_3$) δ 105.1, 86.9, 25.3, 1.1, 0.1. Spectroscopic data was consistent with the values reported in literature.[S6]

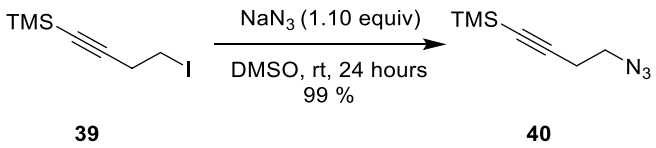

(4-Azidobut-1-yn-1-yl)trimethylsilane (40). Following a slightly modified procedure,[S7] (4-iodobut-1-yn-1-yl)trimethylsilane (**39**) (34.9 g, 138 mmol, 1.00 equiv) was added

to a 0.5 M solution of sodium azide in DMSO (NaN_3, 304 mL, 152 mmol, 1.10 equiv). The reaction mixture was stirred for 24 h at rt, then slowly poured into a mixture of ice/water (800 mL). The aqueous layer was extracted with Et_2O (3 × 300 mL) and the combined organic layers were washed with water (2 × 200 mL), brine (200 mL), dried over $MgSO_4$, filtered and concentrated under reduced pressure. The light yellow crude liquid was purified through a plug of silica, eluting with pentane, to afford pure (4-azidobut-1-yn-1-yl) trimethylsilane (**40**) (22.8 g, 136 mmol, 99% yield) as a colorless liquid. ^{1}H NMR (400 MHz, $CDCl_3$) δ 3.37 (t, J = 6.8 Hz, 2H, $CH_2CH_2N_3$), 2.52 (t, J = 6.8 Hz, 2H, $CH_2CH_2N_3$), 0.15 (s, 9H, TMS); ^{13}C NMR (101 MHz, $CDCl_3$) δ 102.8, 87.3, 49.8, 21.1, 0.0. Spectroscopic data was consistent with the values reported in literature.[S8]

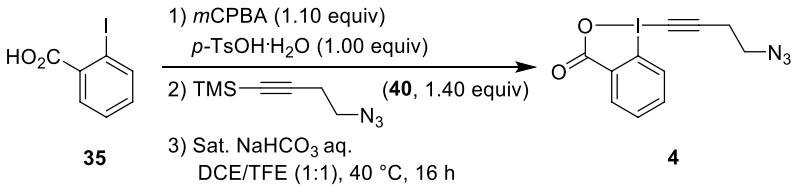

(4-Azidobut-1-ynyl)-1,2-benziodoxol-3(1*H*)-one (4). Following a reported procedure,[S7] 2-iodobenzoic acid (**35**) (24.1 g, 97.0 mmol, 1.00 equiv), *p*-TsOH·H_2O (18.5 g, 97.0 mmol, 1.00 equiv) and *m*CPBA (77%, 23.9 g, 107 mmol, 1.10 equiv) were dissolved in a mixture of DCE (81 mL) and TFE (81 mL). After 1 h stirring at 40 °C, (4-azidobut-1-yn-1-yl)trimethylsilane (**40**) (22.7 g, 136 mmol, 1.40 equiv) was added in one portion. The reaction mixture was stirred for an additional 14 h at the same temperature, then the resulting suspension was filtered and the volatiles were removed under reduced pressure. The resultant residue was dissolved in CH_2Cl_2 (1000 mL) and treated with a solution of sat. $NaHCO_3$ aq. (1000 mL). The mixture was vigorously stirred for 1 h, then the two layers were separated and the aqueous layer was extracted with additional portions of CH_2Cl_2 (3 × 500 mL). The organic layers were combined, dried over $MgSO_4$, filtered and concentrated under reduced pressure. Purification by

column chromatography (SiO_2, EtOAc) afforded (4-azidobut-1-ynyl)-1,2-benziodoxol-3(1*H*)-one (**4**) (5.23 g, 15.3 mmol, 16% yield) as a white solid. R_f 0.47 (EtOAc/MeOH 9:1); ^{1}H NMR (400 MHz, $CDCl_3$) δ 8.37 (d, *J* = 7.5 Hz, 1H, Ar*H*), 8.21 (d, *J* = 7.5 Hz, 1H, Ar*H*), 7.80-7.70 (m, 2H, Ar*H*), 3.56 (t, *J* = 6.5 Hz, 2H, $CH_2CH_2N_3$), 2.86 (t, *J* = 6.5 Hz, 2H, $CH_2CH_2N_3$); ^{13}C NMR (101 MHz, $CDCl_3$) δ 167.2, 134.9, 132.3, 131.6, 131.4, 126.8, 115.8, 104.5, 49.4, 42.7, 21.5. Spectroscopic data was consistent with the values reported in literature.[S9]

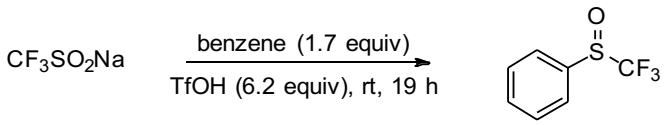

41 **42**

((Trifluoromethyl)sulfinyl)benzene (42). A dry 1 L, three-necked, round-bottomed flask equipped with a thermometer and a mechanical stirrer was charged with sodium trifluoromethanesulfinate (**41**) (90 g, 0.58 mol, 1.0 equiv) and dried under vacuum for 24 h prior to use. The flask was placed in a cold-water bath and trifluoromethanesulfonic acid (0.32 L, 3.6 mol, 6.2 equiv) was added, under argon, in three portions with vigorous stirring (around 100 mL each), in order to keep the temperature under 50 °C. After the addition, the reaction was stirred for 20−30 min until the temperature decreases to rt. Then, benzene (90 mL, 1.0 mol, 1.7 equiv) was added in one portion and the solution was stirred at rt for 19 h under an inert atmosphere. The reaction was quenched by pouring the reaction medium on ice (900 g), extracted with CH_2Cl_2 (3 × 100 mL), and washed with sat. $NaHCO_3$ aq. (3 × 60 mL). The organic phase was dried over $MgSO_4$, filtered, and concentrated under reduced pressure. The product was purified by distillation under reduced pressure (78−80 °C at 15 mmHg) to afford ((trifluoromethyl)-sulfinyl)benzene (**42**) (78 g, 0.40 mol, 69% yield) as a colorless oil. ^{1}H NMR (300 MHz, $CDCl_3$) δ 7.76 (d, *J* = 7.4 Hz, 2H, Ar*H*), 7.70−7.49 (m, 3H, Ar*H*); ^{13}C NMR (75 MHz, $CDCl_3$) δ 135.6 (q, *J* = 1.7 Hz), 133.6, 129.6, 125.9, 124.7 (q, *J* = 335 Hz, CF_3); ^{19}F NMR (282 MHz, $CDCl_3$) δ −75.0 (s, 3F). The characterization data corresponded to the reported values.[S10]

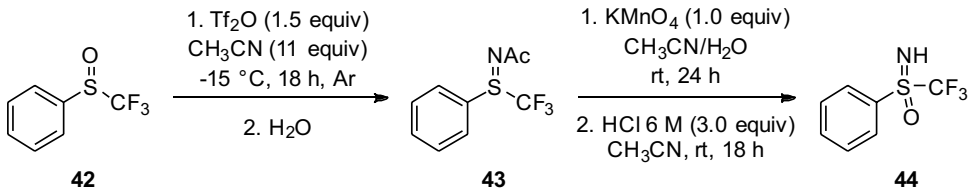

(*S*-(Trifluoromethyl)sulfonimidoyl)benzene (44). In a dry 500 mL two-necked round-bottomed flask equipped with a dropping-funnel and a thermometer, a solution of ((trifluoromethyl)sulfinyl)benzene **42** (40.0 g, 206 mmol, 1.00 equiv) in dry CH_3CN (120 mL, 2.28 mol, 11.0 equiv) was cooled to −15 °C under argon. Tf_2O (52.0 mL, 309 mmol, 1.50 equiv) was introduced into the dropping-funnel and added dropwise to the solution, with the temperature kept around −15 °C. The solution was then left at −15 °C for 18 h under argon in a freezer. The reaction was quenched by pouring the reaction media on ice (400 g), extracted with CH_2Cl_2 (3 × 80 mL), and washed with sat. $NaHCO_3$ aq. (3 × 40 mL). The organic phase was dried over $MgSO_4$, filtered, and concentrated under reduced pressure. To a solution of this crude product in CH_3CN (160 mL) and water (40 mL) was added $KMnO_4$ (32.6 g, 206 mmol, 1.00 equiv) portionwise. The reaction was stirred at rt for 18 h and diluted with H_2O (150 mL), and sat. $Na_2S_2O_4$ aq. was added until complete discoloration of the solution. The product was extracted with CH_2Cl_2 (3 × 70 mL), and the organic phase was dried over $MgSO_4$, filtered, and concentrated under reduced pressure. The crude product was dissolved in CH_3CN (184 mL), and HCl 6 M (67.2 mL) was added. The reaction was stirred at rt for 18 h. Then, water (100 mL) was added and the organic phase was extracted with CH_2Cl_2 (3 × 50 mL), washed with sat. $NaHCO_3$ aq. (3 × 20 mL), dried over $MgSO_4$, filtered, and concentrated under reduced pressure. The product was filtered on silica (200 g) using petroleum ether/EtOAc 8:2 as eluent to afford the (*S*-(trifluoromethyl)sulfonimidoyl)benzene (**44**) (32.8 g, 157 mmol, 76%) as a white solid. ^{1}H NMR (300 MHz, $CDCl_3$) δ 8.15 (d, *J* = 7.5 Hz, 2H, Ar*H*), 7.84−7.72 (m, 1H, Ar*H*), 7.63 (dd, *J* = 8.5, 7.1 Hz, 2H, Ar*H*), 3.53 (s, br s, 1H, N*H*); ^{13}C NMR (75 MHz, $CDCl_3$) δ 135.6,

131.6, 130.7, 129.6, 121.0 (q, J = 333 Hz, CF_3); ^{19}F NMR (282 MHz, $CDCl_3$) δ −79.3 (s, 3F). The characterization data corresponded to the reported values.[S9]

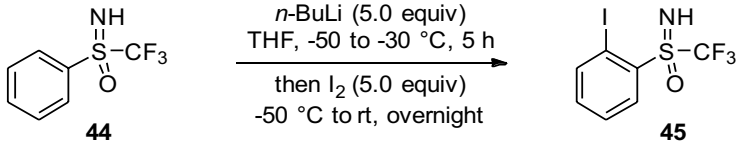

1-Iodo-2-(*S*-(trifluoromethyl)sulfonimidoyl)benzene (45). A solution of 2.5 M *n*-BuLi in hexane (96 mL, 0.24 mol, 5.0 equiv) was added dropwise to a solution of (*S*-(trifluoromethyl)sulfonimidoyl)benzene **44** (10 g, 48 mmol, 1.0 equiv) in freshly distilled THF (300 mL) at -50 °C. The reaction temperature was slowly increased to -30°C over 5 h. The reaction mixture was cooled to -50 °C, and solid I_2 (61 g, 0.24 mol, 5.0 equiv) was added portion-wise. The reaction mixture was allowed to warm to rt overnight and subsequently quenched with sat. NH_4Cl aq. (200 mL). The aqueous layer was extracted with Et_2O (3 × 200 mL), dried with $MgSO_4$, filtered, and concentrated. The residue was purified by flash column chromatography using toluene/MeOH (98:2) as eluent to give 1-iodo-2-(*S*-(trifluoromethyl)sulfonimidoyl)-benzene (**45**) (15 g, 45 mmol, 94% yield) as a pale yellow solid. ^1H NMR (300 MHz, CD_3CN) δ 8.40 (dd, J = 8.1, 1.3 Hz, 1H, Ar*H*), 8.32 (dd, J = 7.9, 0.9 Hz, 1H, Ar*H*), 7.72-7.67 (m, 1H, Ar*H*), 7.43 (td, J = 7.7, 1.5 Hz, 1H, Ar*H*), 4.98 (br. s, 1H, N*H*); ^{13}C NMR (75 MHz, CD_3CN) δ 145.8, 137.2, 135.5, 135.2, 130.5, 121.8 (q, J = 333 Hz), 95.0; ^{19}F NMR (282 MHz, CD_3CN) δ -75.4. The characterization data corresponded to the reported values.[S11]

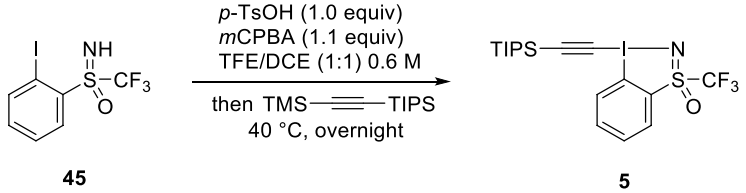

3-(Trifluoromethyl)-1-((triisopropylsilyl)ethynyl)-1*H*-1λ^3,3λ^4-benzo[d][1,3,2] iodathiazole 3-oxide (TIPS-CF_3-EBS, 5). Following a reported procedure,[S12] in a sealed tube 1-

iodo-2-(*S*-(trifluoromethyl)sulfonimidoyl)benzene **45** (1.0 g, 3.0 mmol, 1.0 equiv), *p*-TsOH (0.57 g, 3.0 mmol, 1.0 equiv) and *m*CPBA (0.74 g, 3.3 mmol, 1.1 equiv) were suspended in DCE/TFE (5.0 mL, 1:1) and heated up to 40 °C for 60 min. Triisopropyl ((trimethylsilyl)-ethynyl)silane (1.1 g, 4.2 mmol, 1.4 equiv) was added at this temperature. The reaction mixture was stirred at this temperature overnight. Pyridine (0.34 mL, 4.2 mmol, 1.4 equiv) was added and the mixture was stirred vigorously for 10 min. The reaction mixture was concentrated under vacuum. The crude mixture was dissolved in 5 mL of CH_2Cl_2 and washed with sat. $NaHCO_3$ aq. (3 × 5 mL) and brine (5 mL). The organic layer was dried over $MgSO_4$ and the solvent were evaporated under vacuum. The crude mixture was purified by flash column chromatography using CH_2Cl_2/MeOH 99:1 as mobile phase to afford TIPS-CF_3-EBS (**5**) (1.2 g, 2.2 mmol, 75 % yield) as a slightly yellow solid. ^{1}H NMR (400 MHz, $CDCl_3$) δ 8.79-8.74 (m, 1H, Ar*H*), 8.22 (d, *J* = 7.3 Hz, 1H, Ar*H*), 7.95-7.84 (m, 2H, Ar*H*), 1.15 (m, 21H, TIPS); ^{13}C NMR (101 MHz, $CDCl_3$) δ 135.5, 132.4, 131.4, 129.9, 129.0, 122.6 (q, *J* = 337.2 Hz), 120.9, 110.8, 76.1, 18.7, 11.4; ^{19}F NMR (376 MHz, $CDCl_3$) δ -77.8. The characterization data corresponded to the reported values.[S12]

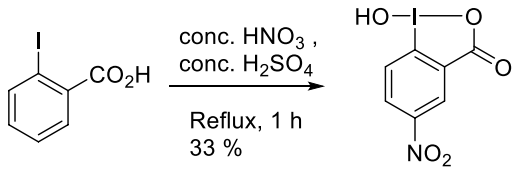

35 **46**

2-Iodosyl-5-nitrobenzoic acid (46). Following a reported procedure,[S3] 2-iodobenzoic acid (**35**) (10.0 g, 40.3 mmol, 1.00 equiv) was suspended in a mixture of fuming nitric acid (6.6 mL) and conc. sulfuric acid (13.4 mL). The reaction was equipped with a cooler, a vapor trap and was heated at 100 °C for 1 h. The reaction mixture was then poured in a mixture of ice/water and the resulting precipitate was filtered. The resulting solid was refluxed in water (100 mL), filtered, washed with acetone (20 mL) and dried under vacuum to afford 2-iodosyl-5-

nitrobenzoic acid (**46**) (4.10 g, 13.2 mmol, 33% yield). ^{1}H NMR (400 MHz, DMSO-d_6) δ 8.69 (dd, J = 8.8, 2.5 Hz, 1H, Ar*H*), 8.54 (d, J = 2.5 Hz, 1H, Ar*H*), 8.08 (d, J = 8.8 Hz, 1H, Ar*H*); ^{13}C NMR (101 MHz, DMSO-d_6) δ 167.7, 148.3, 140.3, 136.0, 129.4, 127.2, 94.3. Spectroscopic data was consistent with the values reported in literature.[S2]

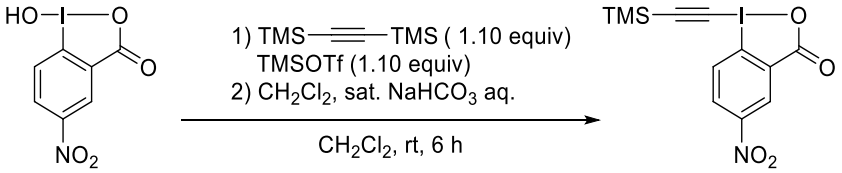

46 **6**

5-Nitro-1-[(trimethylsilyl)ethynyl]-1,2-benziodoxol-3(1*H*)-one (6). Following a reported procedure,[S13] a solution of trimethylsilyl trifluoromethanesulfonate (TMSOTf, 1.29 mL, 7.15 mmol, 1.10 equiv) was added dropwise to a stirred suspension of 2-iodosyl-5-nitrobenzoic acid (**46**) (2.00 g, 6.50 mmol, 1.00 equiv) in CH_2Cl_2 (20 mL) at rt. The mixture was then stirred for 60 min. Bis(trimethylsilyl)acetylene (1.62 mL, 7.15 mmol, 1.10 equiv) was added dropwise to the reaction mixture. After 6 h, sat. $NaHCO_3$ aq. was added (20 mL). The mixture was vigorously stirred for 30 min, then the two layers were separated and the organic layer was washed with additional portions of solution of sat. $NaHCO_3$ aq. (3 × 10 mL). The organic layer was dried over $MgSO_4$, filtered and concentrated under reduced pressure. Recrystallization from CH_3CN (90 mL) afforded 5-nitro-1-[(trimethylsilyl)ethynyl]-1,2-benziodoxol-3(1*H*)-one (**6**) (1.05 g, 2.70 mmol, 42% yield) as a white solid. ^{1}H NMR (400 MHz, $CDCl_3$) δ 9.14 (d, J = 2.5 Hz, 1H, Ar*H*), 8.59 (dd, J = 8.9, 2.5 Hz, 1H, Ar*H*), 8.46 (d, J = 8.9 Hz, 1H, Ar*H*), 0.36 (s, 9H, TMS); ^{13}C NMR (101 MHz, $CDCl_3$) δ 165.3, 151.2, 134.0, 128.8, 128.4, 126.9, 121.8, 118.9, 63.0, -0.3. Spectroscopic data was consistent with the values reported in literature.[S13]

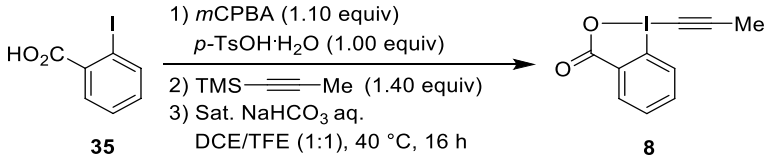

Propynyl-1,2-benziodoxol-3(1*H*)-one (8). Following a reported procedure,[S7] 2-iodobenzoic acid (**35**) (1.42 g, 5.73 mmol, 1.00 equiv), *p*-TsOH·H_2O (1.09 g, 5.73 mmol, 1.00 equiv) and *m*CPBA (77%, 1.41 g, 6.30 mmol, 1.10 equiv) were dissolved in a mixture of CH_2Cl_2 (4.8 mL) and TFE (4.8 mL). After 1 h stirring at 40 °C, trimethyl(prop-1-yn-1-yl)silane (0.900 g, 8.02 mmol, 1.40 equiv) was added in one portion. The reaction mixture was stirred for an additional 14 h at the same temperature, then the resulting suspension was filtered and the volatiles were removed under reduced pressure. The resultant residue was dissolved in CH_2Cl_2 (40 mL) and treated with a solution of sat. $NaHCO_3$ aq. (40 mL). The mixture was vigorously stirred for 1 h, then the two layers were separated and the aqueous layer was extracted with additional portions of CH_2Cl_2 (3 × 30 mL). The organic layers were combined, dried over $MgSO_4$, filtered and concentrated under reduced pressure. Purification by column chromatography (SiO_2, EtOAc) afforded propynyl-1,2-benziodoxol-3(1*H*)-one (**8**) (410 mg, 1.43 mmol, 25% yield) as a white solid. R_f 0.10 (EtOAc); ^{1}H NMR (400 MHz, $CDCl_3$) δ 8.42-8.39 (m, 1H, Ar*H*), 8.22-8.14 (m, 1H, Ar*H*), 7.78-7.73 (m, 2H, Ar*H*), 2.27 (s, 3H, CCCH_3); ^{13}C NMR (101 MHz, $CDCl_3$) δ 167.1, 134.7, 132.2, 131.6, 131.4, 126.6, 115.7, 104.9, 38.5, 5.7. Spectroscopic data was consistent with the values reported in literature.[S7]

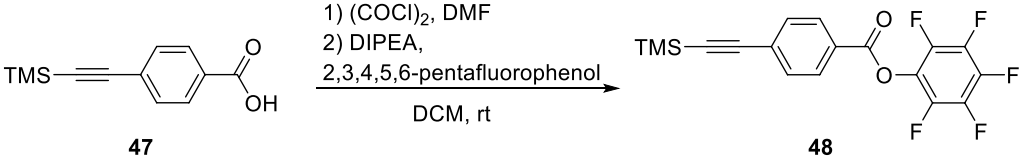

Perfluorophenyl 4-((trimethylsilyl)ethynyl)benzoate (48). Following a reported procedure,[S14] in an oven-dried Schlenk flask, to a solution of 4-((trimethylsilyl)ethynyl)benzoic acid (**47**) (150 mg, 0.687 mmol, 1.00 equiv) in anhydrous CH_2Cl_2 (2.3 mL), oxalyl dichloride (74

μL, 0.86 mmol, 1.3 equiv) and DMF (53 μL, 0.69 mmol, 1.0 equiv) were added at rt. The mixture was stirred for 1 h and concentrated to dryness to yield 4-((trimethylsilyl)ethynyl)-benzoyl chloride, which was used as crude for further synthesis.

To a solution of 4-((trimethylsilyl)ethynyl)benzoyl chloride (54 mg, 0.23 mmol, 1.0 equiv) in CH_2Cl_2 (1 mL) at rt, DIPEA (0.044 mL, 0.25 mmol, 1.1 equiv) and pentafluorophenol (44 mg, 0.24 mmol, 1.05 equiv) were added. The solution was stirred for 2.5 h and directly filtered through a Celite® pad with pentane as eluent. The solvents were then removed under reduced pressure to afford the crude product perfluorophenyl 4-((trimethylsilyl)ethynyl)-benzoate (**48**) (84 mg, 0.22 mmol, 95%) as a white solid. ^{1}H NMR ($CDCl_3$, 400 MHz) δ 8.13 (d, *J* = 8.6 Hz, 2H, C_{Ar}-*H*), 7.61 (d, *J* = 8.5 Hz, 2H, C_{Ar}-*H*), 0.28 (s, 9H, SiCH_3). The characterization data corresponded to the reported values.[S14]

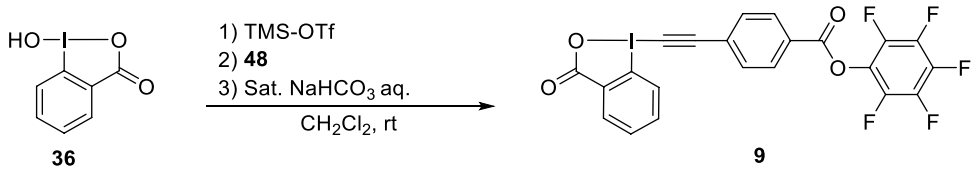

36 **9**

Perfluorophenyl 4-((3-oxo-1λ^3-benzo[d][1,2]iodaoxol-1(3*H*)-yl)ethynyl)benzoate (9). Following a reported procedure,[S14] to a solution of 2-iodosyl benzoic acid (**36**) (264 mg, 0.710 mmol, 1.00 equiv) in CH_2Cl_2 (2.2 mL), TMSOTf (0.15 mL, 0.78 mmol, 1.1 equiv) was added and the reaction was allowed to stir at rt for 1 h, before adding perfluorophenyl 4-((trimethyl-silyl)ethynyl)benzoate (**48**) (300 mg, 0.780 mmol, 1.10 equiv). The reaction was left stirring for 4.5 h and then quenched with sat. $NaHCO_3$ aq. for 15 min. The organic layer was washed with sat. $NaHCO_3$ aq. and the solvents were evaporated under reduced pressure. The crude product was purified by flash column chromatography (1.5% MeOH/CH_2Cl_2) to afford perfluorophenyl 4-((3-oxo-1λ^3-benzo[d][1,2]-iodaoxol-1(3*H*)-yl)- ethynyl)benzoate **9** (293 mg, 0.525 mmol, 74%) as a white solid. ^{1}H NMR ($CDCl_3$, 400 MHz) δ 8.42 (dd, *J* = 7.2, 2.0 Hz,

1H, C_{Ar}-*H*), 8.27-8.24 (m, 3H, C_{Ar}-*H*), 7.83-7.76 (m, 4H, C_{Ar}-*H*). The characterization data corresponded to the reported values.[S14]

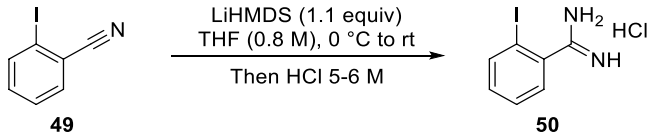

49 **50**

2-Iodobenzamidine hydrochloride (50). Following a reported procedure,[S15] an oven-dried 250 mL flask was charged with LiHMDS (22 mL, 1.0 M, 22 mmol, 1.1 equiv) and cooled to 0 °C and a solution of 2-iodobenzonitrile (**49**) (4.6 g, 20 mmol, 1.0 equiv) in 25 mL of dry THF was added dropwise and the reaction mixture was stirred at this temperature for 15 min. The reaction mixture was then stirred at rt for 4 h. After cooling the reaction mixture to 0 °C, HCl (5 M in isopropanol, 12 mL, 60 mmol, 3.0 equiv) was added dropwise. The reaction mixture was stirred at 0 °C and let warm up to rt. The precipitated product was filtered, washed with Et_2O and dry on the filter for 1 h to afford 2-iodobenzamidine hydrochloride (**50**) (5.1 g, 18 mmol, 90% yield) as a white solid. ^{1}H NMR (400 MHz, DMSO-d_6) δ 8.90 (br s, 4H, N*H*$_2$), 8.01 (dd, *J* = 8.0, 1.0 Hz, 1H, Ar*H*), 7.63-7.49 (m, 2H, Ar*H*), 7.35 (ddd, *J* = 7.9, 7.2, 2.0 Hz,1H, Ar*H*); ^{13}C NMR (101 MHz, DMSO-d_6) δ 167.7, 139.4, 136.0, 132.9, 129.0, 128.4, 94.9. The characterization data corresponded to the reported values.[S16]

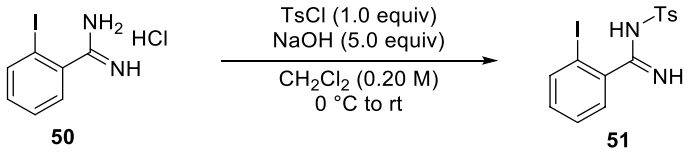

50 **51**

2-Iodo-*N*-tosylbenzimidamide (51). Following a reported procedure,[S12] a round bottom flask was loaded with 2-iodobenzimidamide·HCl (**50**) (2.1 g, 7.4 mmol, 1.0 equiv), *p*-toluene-sulfonyl chloride (1.4 g, 7.4 mmol, 1.0 equiv) and CH_2Cl_2 (37 mL). Subsequently, the solution was cooled down to 0 °C and a 10 M NaOH aq. (3.7 ml, 37 mmol, 5.0 equiv) was added slowly.

The reaction mixture was stirred for 5 h at rt. The mixture was washed with 1M HCl (3 × 20 mL), the organic layer was dried over $MgSO_4$ and concentrated under vacuum The crude mixture was purified by flash column chromatography (pentane/EtOAc 1:2 to 1:1) to afford the 2-iodo-*N*-tosylbenzimidamide (**51**) (2.2 g, 5.5 mmol, 74% yield) as a white solid. ^{1}H NMR (400 MHz, $CDCl_3$) δ 8.37 (br s, 1H, *H*NTs), 7.88 (d, *J* = 8.2 Hz, 2H, Ar*H*), 7.81 (d, *J* = 7.8 Hz, 1H, Ar*H*), 7.37 (qd, *J* = 7.7, 1.5 Hz, 2H, Ar*H*), 7.29 (d, *J* = 8.1 Hz, 2H, Ar*H*), 7.13-7.06 (m, 1H, Ar*H*), 6.05 (br s, 1H, C=N*H*), 2.41 (s, 3H, C*H*$_3$); ^{13}C NMR (101 MHz, $CDCl_3$) δ 165.1, 143.4, 140.2, 139.9, 138.4, 131.9, 129.5, 128.9, 128.5, 127.1, 92.9, 21.7. The characterization data corresponded to the reported values.[S12]

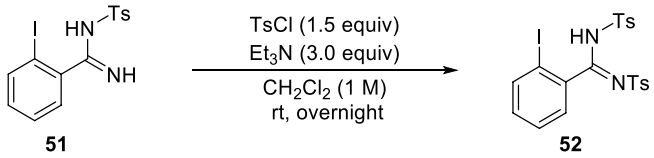

51 52

2-Iodo-*N,N′*-ditosylbenzimidamide (52). Following a slightly modified procedure,[S12] an oven-dried 10 mL microwave vial was charged with 2-iodo-*N*-tosylbenzimidamide (**51**) (1.5 g, 3.8 mmol, 1.0 equiv) and Et_3N (0.80 mL, 5.6 mmol, 1.5 equiv) and 1.9 mL of dry CH_2Cl_2. After 10 min, a solution of *p*-toluenesulfonyl chloride (1.1 g, 5.6 mmol, 1.50 equiv) and Et_3N (0.80 mL, 5.6 mmol, 1.5 equiv) in 1.9 mL of dry CH_2Cl_2 was added dropwise to the reaction mixture. The reaction mixture was stirred at rt overnight. The reaction mixture was then diluted with CH_2Cl_2 (10 mL), and the mixture was washed 1 M HCl (3 × 10 mL). The organic phase was combined with a CH_2Cl_2 extract of the aqueous phase, dried with $MgSO_4$, and concentrated under vacuum. The crude mixture was purified by flash column chromatography using CH_2Cl_2/MeOH 98:2 as mobile phase to afford the 2-iodo-*N,N′*-ditosylbenzimidamide (1.7 g, 3.1 mmol, 83% yield) (**52**) as a yellowish solid. ^{1}H NMR (400 MHz, CD_3CN) δ 9.36 (s, 1H, N*H*), 7.84 (dd, *J* = 8.0, 0.7 Hz, 1H, Ar*H*), 7.62 (br s, 4H, Ar*H*), 7.47 (td, *J* = 7.6, 1.1 Hz, 1H, Ar*H*), 7.36-7.12 (m, 6H), 2.43 (s, 6H, C*H*$_3$); ^{13}C NMR (101 MHz, CD_3CN) δ 161.8, 139.8,

138.6, 132.7, 130.3, 129.8, 128.8, 128.0, 94.1, 21.7.* The characterization data corresponded to the reported values.[S12] * 2 carbons were not resolved by ^{13}C in CD_3CN

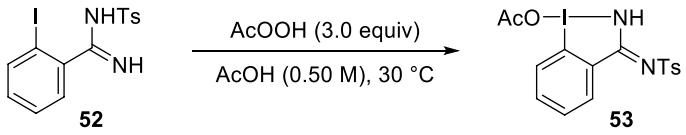

52 53

3-(Tosylimino)-2,3-dihydro-1*H*-1λ^3-benzo[d][1,2]iodazol-1-yl acetate (AcO-H,Ts-BZI, 53). Following a reported procedure,[S12] in a round bottom flask, 2-iodo-*N*-tosyl-benzimidamide **52** (2.0 g, 5.0 mmol, 1.0 equiv) was dissolved in AcOH (10 mL). The reaction mixture was cooled to 0 °C and peracetic acid (39% in acetic acid, 2.6 mL, 15 mmol, 3.0 equiv) was added dropwise to the aluminium foil covered flask. The reaction mixture was stirred at 30 °C for 2 h. The reaction was quenched by the addition of water (5 mL) and the precipitate was filtered and washed with cold water (4 × 5 mL) and with cold Et_2O (3 × 5 mL). The precipitate was dried under vacuum to afford AcO-H,Ts-BZI (**53**) (2.2 g, 4.8 mmol, 97% yield) as a white solid. ^1H NMR (400 MHz, DMSO-d_6) δ 11.97 (s, 1H, N*H*), 8.00 (d, *J* = 7.9 Hz, 1H, Ar*H*), 7.86-7.81 (m, 2H, Ar*H*), 7.73 (d, *J* = 8.2 Hz, 3H, Ar*H*), 7.22 (d, *J* = 8.0 Hz, 2H, Ar*H*), 2.32 (s, 3H, ArCH_3), 1.91 (s, 3H, OCCH_3); ^{13}C NMR (101 MHz, DMSO-d_6) δ 172.1, 169.0, 144.2, 142.5, 140.1, 132.3, 131.9, 129.6, 129.0, 128.5, 126.5, 121.0, 21.1, 20.9. The characterization data corresponded to the reported values.[S12]

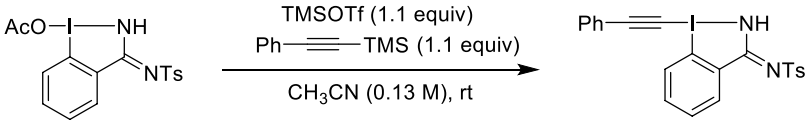

53 10

4-Methyl-*N*-(1-(phenylethynyl)-1,2-dihydro-3*H*-1λ^3-benzo[d][1,2]iodazol-3-ylidene) benzenesulfonamide (Ph-H,Ts-EBZI, 10). Following a slightly modified reported procedure,[S12] an oven-dried round-bottom flask equipped with a magnetic stirring bar was charged

with AcOH,Ts-BZI **53** (1.0 g, 2.2 mmol, 1.0 equiv) and CH_3CN (17 mL). TMSOTf (0.43 mL, 2.4 mmol, 1.1 equiv) was added to the solution and the resulting mixture was stirred at rt for 1 h. Then phenyl((trimethylsilyl)ethynyl)silane (0.61 g, 2.4 mmol, 1.1 equiv) was added to the reaction mixture. After stirring at rt for 18 h, the crude mixture was concentrated under reduced pressure then dissolved in 10 mL of CH_2Cl_2 and 10 mL of sat. $NaHCO_3$ aq. was added and the reaction mixture was vigourously stirred for 30 min. The layers were separated and the organic layer was washed with sat. $NaHCO_3$ aq. (3 × 50 mL) and brine (50 mL) then dried over $MgSO_4$ and concentrated under vacuum. The resulting mixture was triturated in 5 mL of CH_2Cl_2, the precipitate was recovered and dried under vacuum to afford Ph-H,Ts-EBZI (**10**) (0.22 g, 0.44 mmol, 20% yield) as white solid. Mp > 160 °C (decomposition); ^{1}H NMR (400 MHz, $CDCl_3$) δ 8.59 (br s, 1H, N*H*), 8.58-8.53 (m, 1H, Ar*H*), 8.44-8.37 (m, 1H, Ar*H*), 7.88 (d, *J* = 8.1 Hz, 2H, Ar*H*), 7.76-7.69 (m, 2H, Ar*H*), 7.55 (d, *J* = 6.9 Hz, 2H, Ar*H*), 7.42 (m, 3H, Ar*H*), 7.24 (d, *J* = 8.1 Hz, 2H, Ar*H*), 2.38 (s, 3H, C*H*$_3$); ^{13}C NMR (101 MHz, $CDCl_3$) δ 160.0, 142.1, 141.0, 134.4, 133.1, 132.7, 131.5, 130.3, 129.3, 128.8, 127.3, 126.4, 121.4, 114.2, 103.9, 21.6.*; IR (ν_{max}, cm^{-1}) 3336 (w), 3059 (w), 2133 (w), 1574 (m), 1516 (s), 1385 (w), 1269 (m), 1130 (m), 1169 (w), 1080 (m), 876 (m), 737 (m); HRMS (ESI/QTOF) m/z: [M + H]+ Calcd for $C_{22}H_{18}IN_2O_2S^+$ 501.0128; Found 501.0134. * 2C signal not resolved.

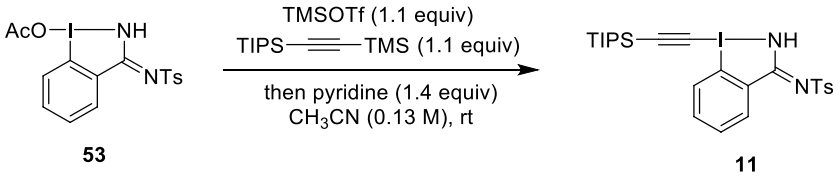

4-Methyl-*N*-(1-((triisopropylsilyl)ethynyl)-1,2-dihydro-3*H*-1λ^3-benzo[d][1,2]iodazol-3-ylidene)benzenesulfonamide (TIPS-H,Ts-EBZI, 11). Following a reported procedure,[S12] an oven-dried round-bottom flask equipped with magnetic stirring bar was charged with AcOH,Ts-BZI **53** (1.0 g, 2.2 mmol, 1.0 equiv) and CH_3CN (17 mL). TMS-OTf (0.43 mL, 2.4

mmol, 1.1 equiv) was added to the solution and the resulting mixture was stirred at rt for 1 h. Then triisopropyl((trimethylsilyl)ethynyl)silane (0.61 g, 2.4 mmol, 1.1 equiv) was added to the reaction mixture. After stirring at rt for 18 h, pyridine (0.25 mL, 3.1 mmol, 1.4 equiv) was added and the reaction mixture was stirred vigorously for 1 h. The crude mixture was filtered and the precipitate washed with CH_3CN. The filtrate was concentrated under vacuum and purified by flash column chromatography using CH_2Cl_2/MeOH 99:1 as mobile phase to afford TIPS-H,Ts-EBZI (**11**) (0.36 g, 0.61 mmol, 28% yield) as a white solid. ^{1}H NMR (400 MHz, $CDCl_3$) δ 8.55 (dd, *J* = 5.8, 3.2 Hz, 2H, N*H* and Ar*H*), 8.48-8.41 (m, 1H, Ar*H*), 7.86 (d, *J* = 8.0 Hz, 2H, Ar*H*), 7.71 (q, *J* = 5.2, 3.5 Hz, 2H, Ar*H*), 7.21 (d, *J* = 8.0 Hz, 2H, Ar*H*), 2.36 (s, 3H, C*H*$_3$), 1.13 (m, 21H, TIPS); ^{13}C NMR (101 MHz, $CDCl_3$) δ 159.9, 142.0, 141.0, 134.1, 133.1, 131.4, 131.3, 129.2, 127.2, 126.4, 113.8, 110.2, 78.1, 21.6, 18.7, 11.4. The characterization data corresponded to the reported values.[S12]

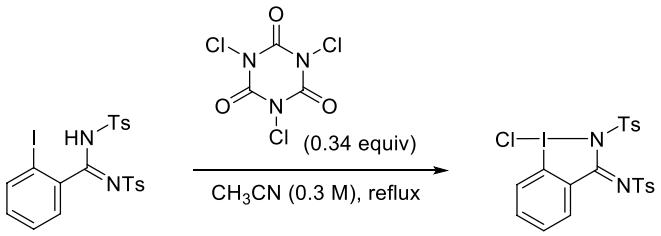

***N*-(1-chloro-2-tosyl-1,2-dihydro-3*H*-1λ^3-benzo[d][1,2]iodazol-3-ylidene)-4-methyl-benzenesulfonamide (Cl-Ts-BZI, 54).** Following a reported procedure,[S12] an oven-dried round-bottom flask equipped with a magnetic stirring bar was charged under Ar with solid 2-iodo-*N,N'*-ditosylbenzimidamide (**52**) (1.1 g, 2.0 mmol, 1.0 equiv) and anhydrous CH_3CN (7.0 mL) was added. The resulting stirred suspension was heated to 75 °C. A solution of trichloroisocyanuric acid (0.19 g, 0.80 mmol, 0.40 equiv, 1.2 equiv in "Cl") in 1.0 mL of anhydrous CH_3CN was added dropwise. After addition was complete, the reaction mixture was refluxed for an additional 15 min. The reaction mixture was vacuum-filtered over a sintered-

glass funnel and the precipitate was rinsed with additional hot CH_3CN (10−20 mL), the precipitate was air-dried. Then the precipitate was washed on a filter with CH_2Cl_2 until only isocyanuric acid was left on the filter. The filtrate was concentrated under vacuum to afford Cl-Ts-BZI (**54**) (1.1 g, 1.9 mmol, 93% yield) as a yellowish solid. ^{1}H NMR (400 MHz $CDCl_3$) δ 9.36 (dd, *J* = 7.4, 2.1 Hz, 1H, Ar*H*), 8.45-8.36 (m, 1H, Ar*H*), 7.88 (ddd, *J* = 6.8, 4.6, 1.7 Hz, 2H, Ar*H*), 7.84 (d, *J* = 8.3 Hz, 2H, Ar*H*), 7.40 (d, *J* = 8.1 Hz, 2H, Ar*H*), 7.32 (d, *J* = 8.3 Hz, 2H, Ar*H*), 6.94 (d, *J* = 8.1 Hz, 2H, Ar*H*), 2.53 (s, 3H, C*H*$_3$), 2.35 (s, 3H, C*H*$_3$); ^{13}C NMR (101 MHz, $CDCl_3$) δ 153.5, 145.3, 143.3, 140.0, 136.7, 136.6, 134.0, 132.2, 130.7, 129.5, 129.4, 129.1, 128.5, 127.0, 114.9, 21.9, 21.8. The characterization data corresponded to the reported values.[S12]

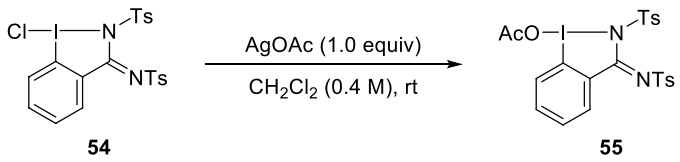

54 **55**

2-Tosyl-3-(tosylimino)-2,3-dihydro-1*H*-1λ^3-benzo[d][1,2]iodazol-1-yl acetate (AcO-Ts-BZI, 55). Following a reported procedure,[S12] an oven-dried round-bottom flask equipped with a magnetic stirring bar was charged under N_2 with Cl-Ts-BZI (**54**) (1.0 g, 1.7 mmol, 1.0 equiv) and 8.0 mL of dry CH_2Cl_2 was added. The flask was covered with aluminium foil to protect it from light. Silver acetate (0.28 g, 1.7 mmol, 1.0 equiv) was added in one portion and the reaction mixture was stirred at rt for 22 h. The solution was filtered over a sintered-glass funnel and washed with CH_2Cl_2. The filtrate was concentrated under vacuum to afford AcO-Ts-BZI (**55**) (1.0 g, 1.7 mmol, quant.) as a white solid. ^{1}H NMR (400 MHz, CD_2Cl_2) δ 9.28 (dd, *J* = 8.0, 1.6 Hz, 1H, Ar*H*), 8.14 (dd, *J* = 8.3, 1.1 Hz, 1H, Ar*H*), 7.87 (td, *J* = 8.4, 7.9, 1.6 Hz, 1H, Ar*H*), 7.83-7.78 (m, 1H, Ar*H*), 7.75 (d, *J* = 8.3 Hz, 2H, Ar*H*), 7.41 (d, *J* = 8.0 Hz, 2H, Ar*H*), 7.33 (d, *J* = 8.4 Hz, 2H, Ar*H*), 6.97 (d, *J* = 8.1 Hz, 2H, Ar*H*), 2.53 (s, 3H, ArC*H*$_3$), 2.36 (s, 3H, ArC*H*$_3$), 2.25 (s, 3H, OCC*H*$_3$); ^{13}C NMR (101 MHz, CD_2Cl_2) δ 176.7, 155.0, 145.7, 143.8,

140.7, 136.8, 136.7, 134.7, 131.8, 131.2, 130.9, 129.8 (×2), 129.3, 127.1, 117.5, 22.0, 21.9, 21.0. The characterization data corresponded to the reported values.[S12]

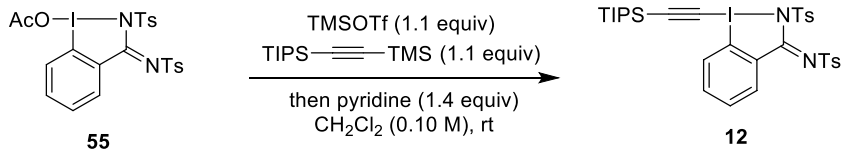

4-Methyl-*N*-(2-tosyl-1-((triisopropylsilyl)ethynyl)-1,2-dihydro-3*H*-1λ^3-benzo[d][1,2] iodazol-3-ylidene)benzenesulfonamide (TIPS-Ts-EBZI, 12). Following a reported procedure,[S12] an oven-dried round-bottom flask equipped with a magnetic stirring bar was charged with AcO-Ts-BZI **55** (0.61 g, 1.0 mmol, 1.0 equiv) and CH_2Cl_2 (7.7 mL). TMSOTf (0.20 mL, 1.1 mmol, 1.1 equiv) was added to the solution and the resulting mixture was stirred at rt for 1 h. Then triisopropyl((trimethylsilyl)ethynyl)silane (0.28 g, 1.1 mmol, 1.1 equiv) was added to the reaction mixture. After stirring at rt for 3 h, pyridine (0.11 mL, 1.4 mmol, 1.4 equiv) was added and the reaction mixture was stirred vigorously for 30 min. The crude mixture was filtered and the precipitate washed with CH_2Cl_2. The filtrate was concentrated under vacuum and purified by flash column chromatography using CH_2Cl_2/MeOH 99.5:0.5 as mobile phase to afford TIPS-Ts-EBZI (**12**) (0.53 g, 0.72 mmol, 72% yield) as a white solid. ^{1}H NMR (400 MHz, $CDCl_3$) δ 9.31 (dd, *J* = 7.9, 1.5 Hz, 1H, Ar*H*), 8.49 (dd, *J* = 8.4, 0.9 Hz, 1H, Ar*H*), 7.86-7.67 (m, 4H, Ar*H*), 7.35 (br d, *J* = 27.6 Hz, 4H, Ar*H*), 6.86 (br s, 2H, Ar*H*), 2.48 (br s, 3H, ArCH_3), 2.30 (br s, 3H, ArCH_3), 1.27-1.10 (m, 21H, TIPS); ^{13}C NMR (101 MHz, $CDCl_3$) δ 153.0, 142.1, 141.1, 139.8, 135.6, 135.1, 134.3, 130.6, 130.5, 127.9 (×2), 127.2 (×2), 125.6, 114.3, 114.2, 67.8, 20.6 (×2), 17.5, 10.2. The characterization data corresponded to the reported values. [S12]

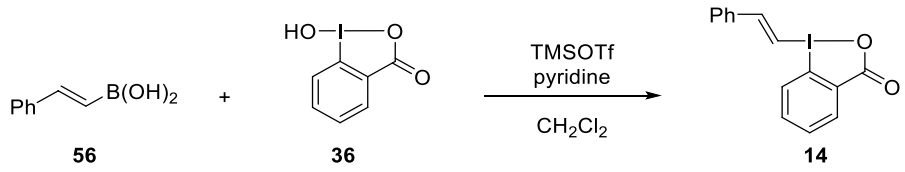

56 **36** **14**

(*E*)-1-Styryl-1λ^3-benzo[*d*][1,2]iodaoxol-3(1*H*)-one (14). To a suspension of 2-iodosyl-benzoic acid (**36**) (343 mg, 1.30 mmol, 1.00 equiv) in dry CH_2Cl_2 (13 mL) was added TMSOTf (0.270 mL, 1.50 mmol, 1.15 equiv) dropwise over 10 min and stirred for 30 min at rt. Afterwards, *trans*-2-phenylvinylboronic acid (**56**) (221 mg, 1.50 mmol, 1.15 equiv) was added and the reaction mixture was stirred until the reaction was completed (1 to 8 h, monitored by TLC, MeOH/ CH_2Cl_2 5:95). Pyridine (0.121 mL, 1.50 mmol, 1.15 equiv) was added and after further stirring for 10 min at rt, the solvent was removed under reduced pressure. The resulting solid was dissolved in CH_2Cl_2 (20 mL) and washed with 1 M HCl (10 mL). The aqueous layer was extracted with CH_2Cl_2 (3 × 20 mL). The organic layers were combined, washed successively with sat. $NaHCO_3$ aq. (40 mL) and water (3 × 20 mL), dried over $MgSO_4$, filtered and the solvent was removed under reduced pressure. The resulting solid was dissolved again in CH_2Cl_2 (minimum amount until dissolution) and precipitated in Et_2O (ca. 150 mL). After precipitation at 4 °C for 2 h, the solid was filtered and washed with Et_2O to afford (*E*)-1-styryl-1λ^3-benzo[*d*][1,2]iodaoxol-3(1*H*)-one (**14**) (351 mg, 1.00 mmol, 77% yield) as a white solid. ^{1}H NMR (400 MHz, CD_3OD) δ 8.32 - 8.25 (m, 1H, Ar*H*), 7.97 (d, *J* = 15.5 Hz, 1H, ICHC*H*Ph), 7.77 - 7.63 (m, 6H, Ar*H* and IC*H*CHPh), 7.54 - 7.45 (m, 3H, Ar*H*); ^{13}C NMR (101 MHz, CD_3OD) δ 170.1, 155.8, 136.7, 135.3, 134.5, 133.3, 132.1, 131.8, 130.2, 129.0, 129.0, 115.5, 100.0. The characterization data corresponded to the reported values.[S17]

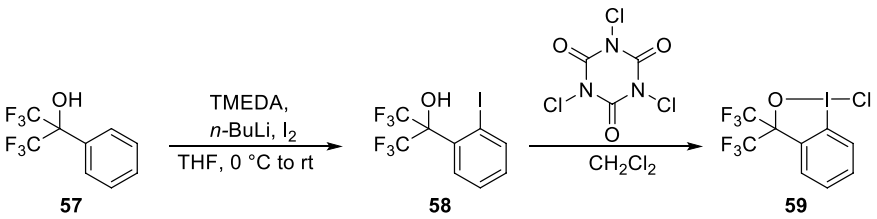

57 58 59

1-Chloro-3,3-bis(trifluoromethyl)-3-(1*H*)-1,2-benziodoxole (59). Following a reported procedure,[S18] tetramethylethylenediamine (TMEDA, distilled over KOH, 1.26 mL, 8.32 mmol, 0.20 equiv) was added to a solution of *n*-BuLi in hexanes (36.6 mL, 91.0 mmol, 2.20 equiv). After 15 min, the solution was cooled to 0 °C and 1,1,1,3,3,3-hexafluoro-2-phenylpropan-2-ol (**57**) (7.00 mL, 41.6 mmol, 1.00 equiv), in THF (37 mL), was added dropwise. The reaction was stirred 30 min at 0 °C, followed by 18 h at rt. Iodine (11.2 g, 44.1 mmol, 1.06 equiv) was added in small portions at 0 °C. The mixture was stirred at 0 °C for 30 min and then at rt for 4 h. The reaction was quenched with a solution of saturated aqueous ammonium chloride (100 mL) and extracted with Et_2O (100 mL). The aqueous layer was then extracted with Et_2O (2 × 50 mL). The organic layers were combined, washed with a solution of saturated aqueous $Na_2S_2O_3$ (2 × 50 mL), dried over $MgSO_4$, filtered and concentrated to afford 1,1,1,3,3,3-hexafluoro-2-(2-iodophenyl)propan-2-ol (**58**) (12.7 g, 34.4 mmol, 82%) as an orange oil which was used without further purification. The crude oil was dissolved in CH_2Cl_2 (34 mL) under air and trichloroisocyanuric acid (2.80 g, 12.0 mmol, 0.35 equiv) was then added portionwise at 0 °C. After 30 min, the resulting suspension was filtered and the filtrate was concentrated *in vacuo*. The resulting solid was dissolved into Et_2O (50 mL), filtered, dried and washed with small amounts of CH_2Cl_2 to afford 1-chloro-3,3-bis-(trifluoromethyl)-3-(1*H*)-1,2-benziodoxole (**59**) (1.59 g, 3.93 mmol, 11%) as a yellow solid. ^{1}H NMR ($CDCl_3$, 400 MHz) δ 8.09 (d, J = 8.5 Hz, 1H, C_{Ar}-*H*), 7.85 (dt, J = 8.6, 4.3 Hz, 1H, C_{Ar}-*H*), 7.73 (d, J = 4.6 Hz, 2H, C_{Ar}-*H*). Spectroscopic data was consistent with the values reported in literature.[S19]

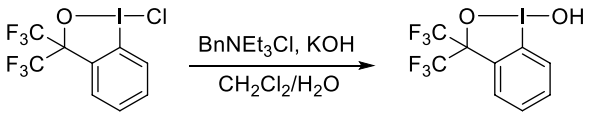

59 60

1-Hydroxy-3,3-bis(trifluoromethyl)-3-(1*H*)-1,2-benziodoxole (60). Following a reported procedure,[S20] benzyltriethylammonium chloride (63 mg, 0.20 mmol, 0.05 equiv) was added to a stirring solution of 1-chloro-3,3-bis(trifluoromethyl)-3-(1*H*)-1,2- benziodoxole (**59**) (1.59 g, 3.93 mmol, 1.00 equiv) in CH_2Cl_2 (27 mL) and KOH (0.22 g, 3.9 mmol, 1.0 equiv) in water (4 mL). The reaction was stirred for 5 h under air. The organic layer was separated, dried over $MgSO_4$ and concentrated *in vacuo*. The resulting solid was purified over a silica plug with EtOAc, then recrystallized in EtOAc and washed with pentane to afford 1-hydroxy-3,3-bis-(trifluoromethyl)-3-(1*H*)-1,2-benziodoxole (**60**) (0.653 g, 1.69 mmol, 43%) as a colorless solid. ^{1}H NMR (DMSO-d_6, 400 MHz) δ 7.81-7.88 (m, 2H, C_{Ar}-*H*), 7.76 (d, *J* = 7.7 Hz, 1H, C_{Ar}-*H*), 7.67 (ddd, *J* = 8.0, 6.7, 1.5 Hz, 1H, C_{Ar}-*H*). Spectroscopic data was consistent with the values reported in literature.[S21]

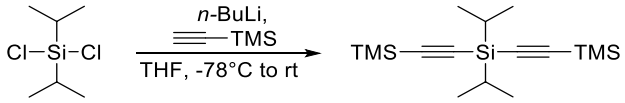

61 62

Diisopropylbis((trimethylsilyl)ethynyl)silane (62). Following a reported procedure,[S14] to a solution of ethynyltrimethylsilane (1.4 mL, 10 mmol, 2.0 equiv) in THF (25 mL) at -78°C, *n*-BuLi (2.5 M in hexane, 4.4 mL, 11 mmol, 2.2 equiv) was added and the mixture was stirred for 10 min at -78 °C and 1 h at rt. Dichlorodiisopropylsilane (**61**) (0.90 mL, 5.0 mmol, 1.0 equiv) was then added and the reaction was allowed to stir overnight at rt. The reaction was quenched with water for 5 min and extracted with Et_2O. The solvents were removed under reduced pressure and the crude product was purified by flash chromatography (pentane) to afford diisopropylbis((trimethylsilyl)ethynyl)silane **62** (0.82 g, 2.6 mmol, 52%) as a colorless

oil. ^{1}H NMR ($CDCl_3$, 400 MHz) δ 1.06 (d, J = 6.4 Hz, 12H, CH(CH_3)$_2$), 0.94-1.03 (m, 2H, CH(CH$_3$)$_2$), 0.18 (s, 18H, Si-CH_3). The characterization data corresponded to the reported values.[S22]

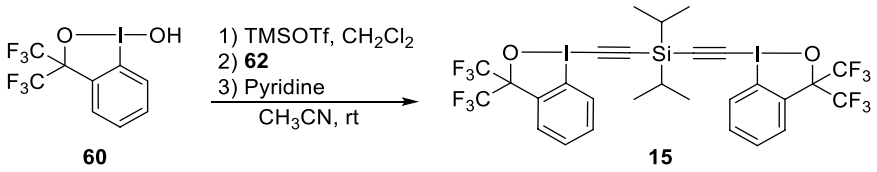

Bis((3,3-bis(trifluoromethyl)-1λ^3-benzo[d][1,2]iodaoxol-1(3*H*)-yl)ethynyl)diisopropylsilane (15). Following a reported procedure,[S14] to a solution of 1-hydroxy-3,3-bis-(trifluoromethyl)-3-(1*H*)-1,2-benziodoxole (**60**) (0.20 g, 0.52 mmol, 2.5 equiv) in CH_2Cl_2 (6.6 mL), TMSOTf (0.10 mL, 0.52 mmol, 2.5 equiv) was added and the mixture was allowed to stir for 20 min at rt. The solvents were then removed under reduced pressure and the solid was redissolved in CH_3CN (4.0 mL) and diisopropylbis((trimethylsilyl)ethynyl)silane (**62**) (0.064 g, 0.21 mmol, 1.0 equiv) was added. After 20 min pyridine (0.025 mL, 0.31 mmol, 2.5 equiv) was added and the reaction was stirred for 20 min, the solvents were then evaporated under reduced pressure and the solid was partitioned between CH_2Cl_2 and water. The organic layer was then washed with sat. $NaHCO_3$ aq. and the solvents were removed under reduced pressure. The crude product was purified by flash chromatography (CH_2Cl_2) to yield bis((3,3-bis(trifluoromethyl)-1λ^3-benzo[d][1,2]iodaoxol-1(3*H*)-yl)ethynyl)diisopropylsilane (**15**) (0.128 g, 0.142 mmol, 69%) as a white solid. ^{1}H NMR ($CDCl_3$, 400 MHz) δ 8.28 (d, J = 8.2 Hz, 2H, C_{Ar}-*H*), 7.84 (d, J = 7.6 Hz, 2H, C_{Ar}-*H*), 7.70 (t, J = 7.4 Hz, 2H, C_{Ar}-*H*), 7.64 (td, J = 7.8, 7.3, 1.6 Hz, 2H, C_{Ar}-*H*), 1.21 (m, 14H, Si-C*H*, Si-CHCH_3). The characterization data corresponded to the reported values.[S14]

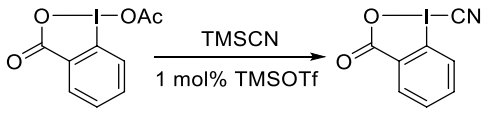

37 **18**

1-Cyano-1,2-benziodoxol-3-(1*H*)-one (18). Following a reported procedure,[S23] 1-acetoxy-1,2-benziodoxol-3-(1*H*)-one **37** (11.8 g, 38.6 mmol, 1.00 equiv) was dissolved under nitrogen in dry CH_2Cl_2 (200 mL). To the clear colorless solution was added *via* syringe TMSCN (10 mL, 77 mmol, 2.00 equiv) over 5 min, then TMSOTf (70 µL, 0.386 mmol, 0.01 equiv). Precipitation occurred within 5 min and the reaction mixture was stirred at rt and under nitrogen for 30 min to ensure the completion of the reaction. The resulting thick white suspension was diluted with hexane (5 mL) before being filtered and the solid was washed with hexane (3 × 20 mL) and dried *in vacuo* affording 1-cyano-1,2-benziodoxol-3-(1*H*)-one **18** (10.3 g, 37.7 mmol, 98 %) as a white solid. ^{1}H NMR (DMSO-d_6, 400 MHz) δ 8.29 (d, J = 8.3 Hz, 1 H, Ar*H*), 8.13 (dd, J = 7.4, 1.7 Hz, 1 H, Ar*H*), 8.06-7.97 (m, 1 H, Ar*H*), 7.88 (t, J = 7.3 Hz, 1 H, Ar*H*); ^{13}C NMR (DMSO-d_6, 100 MHz) δ 166.7, 136.5, 132.0, 131.9, 130.2, 127.8, 117.5, 87.9. The characterization data corresponded to the reported values.[S18]

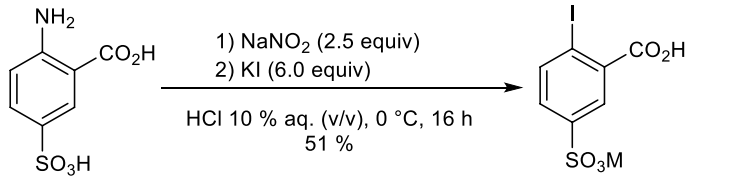

63 **64** M = K, Na

Potassium 3-carboxy-4-iodobenzenesulfonate (64). Following a reported proce dure,[S24] 2-amino-5-sulfobenzoic acid (**63**) (4.34 g, 20.0 mmol, 1.0 equiv) was suspended in a 10% HCl aq. (100 mL) and cooled to 0 °C. A cooled solution of $NaNO_2$ (3.45 g, 50.0 mmol, 2.5 equiv) in water (18 mL) was slowly added over 45 min. After an additional 30 min stirring at this temperature, a cooled solution of KI (19.9 g, 120 mmol, 6.0 equiv) in water (75 mL) was slowly added over 1 h at 0 °C. The resulting dark solution was allowed to warm to rt and stirred

for 16 h. Then, the reaction was slowly quenched by small portions of $NaHSO_3$ (around 14 g) until the solution persistently turned as a light-yellow suspension. The resulting suspension was filtered, washed with acetone (3 × 100 mL) and CH_2Cl_2 (50 mL) to afford a yellow pale solid. The collected solid was then recrystallized from water and washed with cold water (2 × 50 mL), acetone (2 × 50 mL) and CH_2Cl_2 (2 × 50 mL) to yield pure potassium 3-carboxy-4-iodobenzenesulfonate **64** (3.71 g, 10.1 mmol, 51% yield) as a pale-yellow solid. ^{1}H NMR (400 MHz, DMSO-d_6) δ 7.95 (d, J = 8.1 Hz, 1H, ArH), 7.90 (d, J = 2.0 Hz, 1H, ArH), 7.41 (dd, J = 8.1, 2.1 Hz, 1H, ArH); ^{13}C NMR (101 MHz, DMSO-d_6) δ 167.9, 147.8, 140.5, 136.4, 129.5, 127.3, 94.8. Spectra data was consistent with the values reported in literature.[S2]

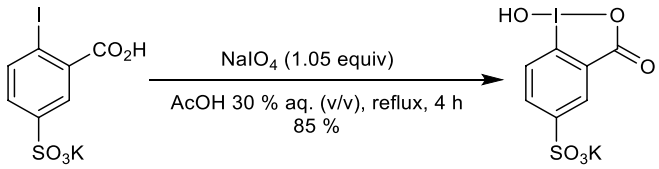

Potassium 1-hydroxy-3-oxo-1,3-dihydro-1λ^3-benzo[d][1,2]iodaoxole-5-sulfonate (65). Following a modified reported procedure,[S25] potassium 3-carboxy-4-iodo- benzene-sulfonate **64** (1.75 g, 8.17 mmol, 1.00 equiv) and $NaIO_4$ (2.85 g, 7.78 mmol, 1.05 equiv) were suspended in 30% AcOH aq. (14 mL). The vigorously stirred mixture was heated and refluxed under air for 4 h. The reaction mixture was allowed to cool to rt and placed under vacuum. The resulting precipitate was filtered and washed with acetone (3 × 100 mL) and CH_2Cl_2 (100 mL). The collected solid was dissolved in MeOH, filtered and concentrated under pressure to afford pure potassium 2-iodosyl-5-sulfobenzoate, **65** (2.52 g, 6.59 mmol, 85% yield) as a white solid. Mp 299–300 °C; ^{1}H NMR (400 MHz, DMSO-d_6) δ 8.18 (d, J = 1.8 Hz, 1H, ArH), 8.12 (dd, J = 8.3, 1.9 Hz, 1H, ArH), 7.80 (d, J = 8.3 Hz, 1H, ArH); ^{13}C NMR (101 MHz, DMSO-d_6) δ 167.5 (C=O), 151.1 (ArC), 132.1 (ArC), 130.7 (ArC), 128.5 (ArC), 126.3 (ArC), 119.1 (ArC);

IR ν_{max} 1648 (*m*), 1618 (*m*), 1205 (*s*), 1095 (*m*), 1041 (*m*), 1011 (*m*); HRMS (ESI/QTOF) m/z: $[M-K]^-$ Calcd for $C_7H_4IO_6S^-$ 342.8779; Found 342.8779.

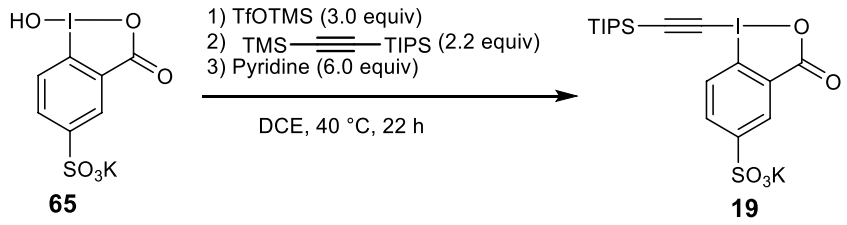

Potassium 3-oxo-1-((triisopropylsilyl)ethynyl)-1,3-dihydro-1λ^3-benzo[d][1,2] iodaoxole-5-sulfonate (19). TMSOTf (2.55 mL, 14.1 mmol, 3.0 equiv) was added dropwise to a stirred suspension of potassium 2-iodosyl-5-sulfobenzoate (**65**) (1.80 g, 4.71 mmol, 1.0 equiv) in CH_2Cl_2 (157 mL) at 40 °C. After 2 h stirring at this temperature, triisopropyl ((trimethylsilyl)ethynyl)silane (2.64 g, 10.4 mmol, 2.2 equiv) was slowly added to the solution. The reaction mixture was stirred for another 18 h and pyridine (2.29 mL, 28.3 mmol, 6.0 equiv) was added. After 2 additional hours stirring, the mixture was diluted with CH_2Cl_2 (200 mL), washed with a 0.5 M sat. $NaHCO_3$ aq. (150 mL) and a 0.5 M HCl aq. (150 mL). The organic layer was dried over $MgSO_4$, filtered and the volatiles were removed *in vacuo*. The crude orange oil was purified by column chromatography (SiO_2, CH_2Cl_2/MeOH gradient from 9:1 to 8:2) to yield pure K/Na-5-sulfonate TIPS-EBX-SO_3M **19** (2.00 g, 3.66 mmol, 78% yield) as a white solid. Yield for **19** calculated based on K salt. R_f 0.50 (CH_2Cl_2/MeOH, 4:1); Mp 325–326 °C; ^{1}H NMR (400 MHz, DMSO-d_6) δ 8.30 (d, J = 2.0 Hz, 1H, Ar*H*), 8.26 (d, J = 8.5 Hz, 1H, Ar*H*), 7.98 (dd, J = 8.5, 2.1 Hz, 1H, Ar*H*), 1.24 – 1.00 (m, 21H, TIPS); ^{13}C NMR (101 MHz, DMSO-d_6) δ 165.9 (C=O), 151.7 (ArC), 132.2 (ArC), 131.2 (ArC), 128.3 (ArC), 126.6 (ArC), 115.4 (ArC), 110.7 (CC), 67.1 (CC), 18.4 (CH_3), 10.7 (CH); IR ν_{max} 2952 (*w*), 2866 (*w*), 2372 (*w*), 2347 (*w*), 2325 (*w*), 1634 (*s*), 1238 (*s*), 1169 (*s*), 1102 (*m*), 1036 (*s*), 994 (*m*), 882 (*m*); HRMS (ESI/QTOF) m/z: $[M-K]^-$ Calcd for $C_{18}H_{24}IO_5SSi^-$ 507.0164; Found 507.0165; ICP-MS 53.66 µg/mg Na, 5.15 µg/mg K.

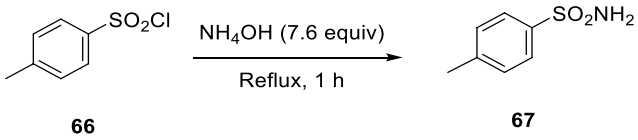

66 67

4-Methylbenzenesulfonamide (67). Following a reported procedure,[S14] in a 100 mL round-bottom flask, a solution of 4-methylbenzene-1-sulfonyl chloride (**66**) (4.00 g, 21.0 mmol, 1.00 equiv) in NH_4OH solution 25% w/w (25.0 mL, 161 mmol, 7.70 equiv) was heated to reflux for 1 h. After reaction completion, the reaction mixture was cooled down and filtered. The crude product was recrystallized in water to afford 4-methylbenzenesulfonamide (**67**) as white crystalline solid (2.81 g, 16.4 mmol, 78%). ^{1}H NMR (400 MHz, $CDCl_3$) δ 7.82 (d, J = 8.3 Hz, 2H, Ar*H*), 7.32 (d, J = 8.0 Hz, 2H, Ar*H*), 4.77 (br s, 2H, NH_2), 2.43 (s, 3H, ArCH_3). The characterization data corresponded to the reported values.[S19]

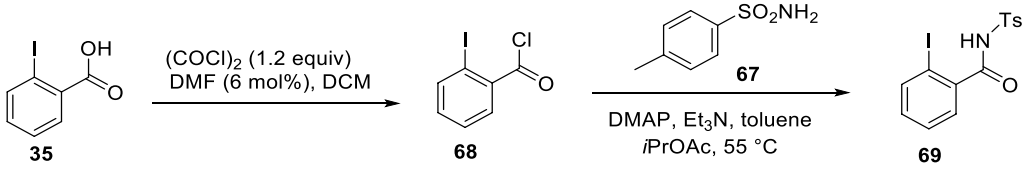

35 68 69

2-Iodo-*N*-tosylbenzamide (69). In a 25 mL round-bottom flask, 2-iodobenzoic acid (**35**) (2.48 g, 10.0 mmol, 1.00 equiv) and DMF (1 drop, ~6 mol%) were suspended in CH_2Cl_2 (7.0 mL). Oxalyl chloride (1.1 mL, 12 mmol, 98 %, 1.2 equiv) was added dropwise at 0 °C. After the addition, the reaction was warmed up to rt and stirred for 3 h. The solvent and the oxalyl chloride excess were removed in vacuum. The crude 2-iodobenzoyl chloride was dissolved in toluene (6.5 mL) and transferred to a solution of 4-methylbenzenesulfonamide (**67**) (1.50 g, 8.15 mmol, 0.820 equiv), DMAP (5.5 mg, 0.05 mmol, 0.005 equiv), and Et_3N (3.2 mL, 23 mmol, 2.3 equiv) in *i*PrOAc (20 mL). The reaction mixture was heated to 55 °C and stirred for 1 h. Water (10 mL) was added to quench the excess of acyl chloride. The organic layer was washed with 0.7 M HCl aq. (70 mL) and the aqueous layer was extracted with EtOAc (2 × 100 mL). The organic layers were combined, dried and the solvent was removed under reduced

pressure. The crude product was purified by flash chromatography using EtOAc/Pentane 1:3.5 as mobile phase to afford 2-iodo-*N*-tosylbenzamide (**69**) as a slightly brown gum (2.92 g, 7.27 mmol, 80%). ^{1}H NMR (400 MHz, $CDCl_3$) δ 9.04 (s, 1H, N*H*), 7.98 (d, *J* = 8.3 Hz, 2H, Ar*H*), 7.76 (d, *J* = 7.9 Hz, 1H, Ar*H*), 7.34 (m, 4H, Ar*H*), 7.10 – 7.03 (m, 1H, Ar*H*), 2.43 (s, 3H, ArCH_3); ^{13}C NMR (101 MHz, $CDCl_3$) δ 165.9, 145.4, 140.2, 138.4, 135.3, 135.0, 132.5, 129.6, 128.9, 128.3, 91.8, 21.8. The characterization data corresponded to the reported values.[S19]

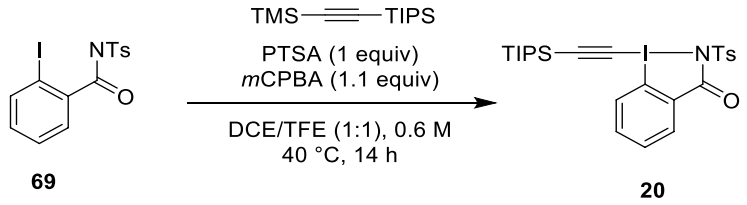

69 **20**

***N*-[Tolylsulfonyl]-1-[triisopropylsilylethynyl]-1,2-benziodazol-3(1*H*)-one (20).** In a 5 mL microwave reaction vial, 2-iodo-*N*-tosylbenzamide **69** (1.00 g, 2.49 mmol, 1.00 equiv), *p*-toluenesulfonic acid (430 mg, 2.49 mmol, 1.00 equiv) and *meta*-chloroperbenzoic acid (677 mg, 2.74 mmol, 1.10 equiv) were dissolved in CH_2Cl_2/TFE mixture (1:1, 0.6 M). The solution was stirred for 1 h at 40 °C. Triisopropyl((trimethylsilyl)ethynyl)silane (888 mg, 3.49 mmol, 1.40 equiv) was then added and the reaction mixture was stirred at 40 °C overnight. The precipitate was dissolved in CH_2Cl_2 (25 mL) and the organic layer was washed with sat. $NaHCO_3$ aq. (2 × 20 mL) and with brine (15 mL). The combined aqueous layers were extracted with CH_2Cl_2 (2 × 20 mL). The organic layers were combined, dried with Na_2SO_4, filtered and evaporated under reduced pressure. The crude reaction mixture was purified by recrystallization in EtOAc (35 mL) to afford *N*-[tolylsulfonyl]-1-[triisopropylsilylethynyl]-1,2-benziodazol-3(1*H*)-one (**20**) (1.39 g, 2.38 mmol, 96% yield) as white crystals. ^{1}H NMR (400 MHz, $CDCl_3$) δ 8.40 – 8.34 (m, 1H, Ar*H*), 8.32 – 8.27 (m, 1H, Ar*H*), 8.01 (d, *J* = 8.3 Hz, 2H, Ar*H*), 7.70 (dd, *J* = 6.5, 3.5 Hz, 2H, Ar*H*), 7.28 (d, *J* = 8.2 Hz, 2H, Ar*H*), 2.38 (s, 3H, CH_3), 1.15 (m, 21H, TIPS); ^{13}C NMR (100 MHz, $CDCl_3$) δ 160.7, 143.4, 137.9, 135.2, 134.3, 132.0, 131.6, 129.2,

128.0, 127.1, 115.0, 114.0, 70.6, 21.6, 18.6, 11.2. The characterization data corresponded to the reported values.[S19]

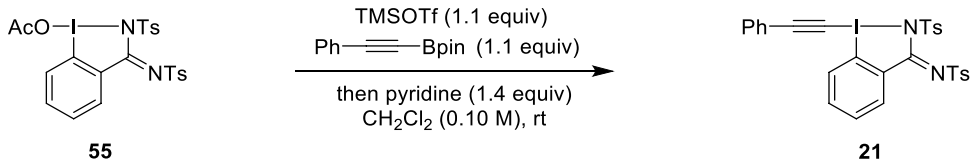

(*E*)-4-methyl-*N*-(1-(phenylethynyl)-2-tosyl-1,2-dihydro-3*H*-1λ^3-benzo[d][1,2] iodazol-3-ylidene)benzenesulfonamide (Ph-Ts-EBZI, 21). Following a reported procedure, [S12] an oven-dried round-bottom flask equipped with a magnetic stirring bar was charged with AcO-Ts-BZI **55** (0.40 g, 0.65 mmol, 1.0 equiv) and CH_2Cl_2 (5.0 mL). TMSOTf (0.13 mL, 0.72 mmol, 1.1 equiv) was added to the solution and the resulting mixture was stirred at rt for 1 h. Then 2-phenyl-1-ethynylboronic acid pinacol ester (0.18 g, 0.72 mmol, 1.1 equiv) was added to the reaction mixture. After stirring at rt for 2 h, pyridine (74 µL, 0.91 mmol, 1.4 equiv) was added and the reaction mixture was stirred vigorously for 1 h. The crude mixture was filtered and the precipitate washed with CH_2Cl_2. The filtrate was concentrated under vacuum and purified by flash column chromatography using CH_2Cl_2/MeOH 99.5:0.5 as mobile phase. Recrystallization in EtOAc afforded the Ph-Ts-EBZI (**21**) as a white solid (0.17 g, 0.26 mmol, 40% yield). R_f = 0.30 (CH_2Cl_2/MeOH 1%); Mp > 190 °C (decomposition); ^{1}H NMR (400 MHz, $CDCl_3$) δ 9.33 (dd, *J* = 7.88, 1.43 Hz, 1H, Ar*H*), 8.44 (d, *J* = 7.73 Hz, 1H, Ar*H*), 7.88-7.69 (br m, 5H, Ar*H*), 7.64-7.56 (m, 2H, Ar*H*), 7.51 (dd, *J* = 8.50, 6.31 Hz, 1H, Ar*H*), 7.44 (t, *J* = 7.32 Hz, 2H, Ar*H*), 7.41-7.28 (br m, 3H, Ar*H*), 6.87 (br s, 2H, Ar*H*), 2.49 (br s, 3H), 2.33 (br s, 3H); ^{13}C NMR (101 MHz, $CDCl_3$) δ 154.1, 143.4, 142.2, 141.0, 136.7, 136.1, 135.7, 133.1, 131.8, 131.5, 131.1, 129.0, 128.9, 128.5, 128.4, 126.8, 120.4, 115.8, 107.6, 55.1, 21.7 (×2); IR (νmax, cm^{-1}) 3065 (w), 2983 (w), 2915 (w), 2144 (w), 1736 (w), 1524 (m), 1447 (w), 1350 (w), 1282 (m), 1146 (m), 1079 (s), 949 (w), 847 (m), 806 (m), 715 (s), 653 (s); HRMS (ESI/QTOF) m/z: $[M + H]^+$ Calcd for $C_{29}H_{24}IN_2O_4S_2^+$ 655.0217; Found 655.0229.

2.3. Synthesis of Other Irreversible Covalent Reagents

Super-cinnamaldehydes. Compounds **1** and **3** were synthesized and purified according to reported procedures.[S26]

2-Sulfopyridines. Compounds **22** and **23** were synthesized and purified according to reported procedures.[S27]

Heteroaromatic sulfones. Compounds **16, 17** and **24** were synthesized and purified according to reported procedures.[S28]

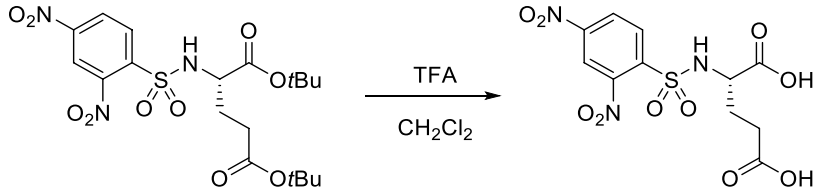

70 **7**

Compound **70** was synthesized and purified according to procedures described in ref. [S29].

Compound **7**. To a solution of **70** (35.2 mg, 71.9 μmol) in CH_2Cl_2 (0.18 mL), TFA (0.18 mL) was added dropwise at rt. After the mixture was stirred for 9 h, the solution was diluted with Et_2O and concentrated. The residue was dissolved in a minimum amount of CH_2Cl_2, and Et_2O was added to form a white precipitate. The supernatant was removed, and the solid was triturated in Et_2O (×2). The obtained solid was dissolved in H_2O and lyophilized to give compound **7** (5.2 mg, 19% yield) as a white solid. Mp 66-68 °C; $[\alpha]_D^{20}$ -18 (*c* 0.20, MeOH); IR (neat): 3102 (m), 1710 (s), 1607 (m), 1538 (s), 1412 (m), 1348 (s), 1306 (w), 1167 (s), 1104 (m), 982 (w), 903 (m), 834 (m), 747 (s), 664 (m), 615 (m); ^{1}H NMR (400 MHz, CD_3OD) δ 8.72 (d, $^4J_{HH}$ = 2.3 Hz, 1H), 8.58 (dd, $^3J_{HH}$ = 8.7, $^4J_{HH}$ = 2.3 Hz, 1H), 8.33 (d, $^3J_{HH}$ = 8.7 Hz, 1H), 4.19 (dd, $^3J_{HH}$ = 9.9, 4.6 Hz, 1H), 2.49 – 2.40 (m, 2H), 2.21 (m, 1H), 1.97 – 1.83 (m, 1H); ^{13}C NMR (101 MHz, CD_3OD) δ 176.1 (C), 173.9 (C), 151.4 (C), 149.3 (C), 140.4 (C), 133.5 (CH),

127.9 (CH), 121.3 (CH), 57.1 (CH), 30.7 (CH_2), 28.6 (CH_2); HRMS (ESI, +ve) calcd for $C_{11}H_{11}N_3O_{10}S$ ($[M+Na]^+$): 400.0058, found: 400.0047.

3. Cell Culture

Human cervical cancer-derived HeLa Kyoto cells were cultured in DMEM (GlutaMAX, 4.5 g/L D-glucose, with phenol red) medium containing 10% fetal bovine serum (FBS) and 1% Penicillin/Streptomycin (PS). The cells were grown at 37 °C under 5% CO_2 on a 25 cm^3 tissue culture flask (TPD Corporation). Cells were detached by treatment with 1.5 mL of TrypLE Express at 37 °C for 5 min, followed by the addition of 6 mL of DMEM (GlutaMAX, 4.5 g/L D-glucose, with phenol red) medium at 37 °C. The cells were resuspended in DMEM (GlutaMAX, 4.5 g/L D-glucose, with phenol red) medium and plated according to the concentration needed.

4. High-Content High-Throughput (HCHT) Inhibitor Screening

4.1. General Procedure for HCHT Inhibitor Screening

4.1.1. Pre-Incubation of Inhibitors

HeLa Kyoto cells were seeded at 1.2 ×10^4 cells/well in FluoroBrite DMEM + 10% FBS on µ-Plate 96-well Black ibiTreat sterile and kept at 37 °C with 5% CO_2 overnight. The next day, serial dilutions of the inhibitors in PBS (10× final concentration), reporter **26** (100 µM in PBS) and a solution of Hoechst 33342 (100 µg/mL) and PI (10 µg/mL) in PBS were prepared freshly in a 96-well V-bottom plate. Then, cells were washed with PBS (3 × 3 mL/well) and the media was exchanged to FluoroBrite DMEM (4 × 150 µL/well) using a plate washer (Biotek EL406®), keeping always a final volume of 135 µL/well. The inhibitor solutions from the V-bottom plate were added to the cells (15 µL/well, 10× final concentration in PBS) using an electronic multichannel pipette to reach a final volume of 150 µL/well. Cells were incubated for the time of interest (for details of each inhibitor, see **Section 4.2**) at 37 °C with 5% CO_2. After this, cells were washed again using the plate washer, and reporter solution **26** from the V-bottom plate was added (15 µL/well) using an electronic multichannel pipettes to reach a final volume of 150 µL/well and a final concentration of 10 µM, except for the control wells, where only PBS was added (15 µL/well). After 30 min of incubation at 37 °C with 5% CO_2, the plate was washed again using the plate washer. Then, the solution of Hoechst 33342 and PI from the V-bottom plate was added (15 µL/well) using an electronic multichannel pipette to reach a final volume of 150 µL/well. After 15 min of incubation at 37 °C with 5% CO_2, the plate was washed one last time and the cells were kept in clean FluoroBrite DMEM. During imaging, samples were kept at 37 °C with 5% CO_2 in the microscope.

4.1.2. Co-Incubation of Inhibitors and Reporters

HeLa Kyoto cells were seeded at 1.2 ×10^4 cells/well in FluoroBrite DMEM + 10% FBS on µ-Plate 96-well Black ibiTreat sterile and kept at 37 °C with 5% CO_2 overnight. The next day, serial dilutions of the inhibitors in PBS (10x final concentration), reporter **26** (110 µM in PBS) and a solution of Hoechst 33342 (100 µg/mL) and PI (10 µg/mL) in PBS were prepared freshly in a 96-well V-bottom plate. Then, cells were washed with the plate washer. The inhibitor solutions from the V-bottom plate were added to the cells (15 µL/well, 10× final concentration in PBS) using an electronic multichannel pipette to reach a final volume of 150 µL/well. Cells were incubated for the time of interest (for details of each inhibitor, see **Section 4.2**) at 37 °C with 5% CO_2. Reporter solution **26** from V-bottom plate was then added (15 µL/well) using an electronic multichannel pipette to reach a final volume of 165 µL/well and a final concentration of 10 µM 30 min before the next washing process, except for the control wells, where only PBS was added (15 µL/well). The plate was washed again using the plate washer. The solution of Hoechst 33342 and PI from the V-bottom plate was added (15 µL/well) using an electronic multichannel pipette to reach a final volume of 150 µL/well. After 15 min of incubation at 37 °C with 5% CO_2, the plate was washed one last time and the cells were kept in clean FluoroBrite DMEM. During imaging, samples were kept at 37 °C with 5% CO_2 in the microscope.

Note: For each of both pre-incubation and co-incubation experiment, 4 images at 10× were recorded per well using three channels: blue for Hoechst 33342 (excitation filter: 377/50 nm; emission filter: 477/60 nm), green for FITC reporters (excitation filter: 475/34 nm; emission filter: 536/40 nm) and red for PI (excitation filter: 531/40 nm ; emission filter: 593/40 nm). Dulipicates were performed for each condition.

4.2. HCHT Inhibitor Screening

Inhibitor screening followed the previously reported protocol.[S30] In brief, integrated fluorescent intensity values (per cell) for each condition in the presence of compounds were normalized to the same parameter for condition with the reporter **26** alone (no inhibitor, I_{rel} = 1) or for the condition with no reporter **26** (I_{rel} = 0; Hoechst 33342 and PI only), for each set of experiments. Duplicates were performed for each condition. The resulting dependence of the relative fluorescent intensity values (I_{rel}) to the concentration of inhibitors ($c_{inhibitor}$) was plotted and fitted with Equation (S1) to retrieve the half-maximal inhibitory concentration (IC_{50}) value and the Hill coefficient (n).

$$I_{rel} = 1 / (1 + (IC_{50} / c_{inhibitor})^{-n}) \qquad (S1)$$

Hoechst 33342 is a cell-permeable DNA stain that is used to label all cells, propidium iodide (PI) is a membrane-impermeable intercalator that is used to differentiate necrotic and apoptotic cells from healthy cells. Relative cell viability (RV) for each condition in the presence of inhibitors was calculated as the count of Hoechst 33342 stained cells minus the count of PI stained cells divided by the count of Hoechst 33342 stained cells only, for each set of experiments. Duplicates were performed for each condition. The resulting dependence of the relative cell viability (RV_{rel}) to the concentration of inhibitors ($c_{inhibitor}$) was plotted and fitted with Equation (S2) to retrieve the concentration causing 50% cell growth inhibition (GI_{50}) value and the Hill coefficient (n).

$$RV_{rel} = 1 / (1 + (GI_{50} / c_{inhibitor})^{-n}) \qquad (S2)$$

Note: Reporter **26** was not toxic for 1 h at 10 μM. Also in this study, the count value of living cells with the addition of reporter **26**, Hoechst 33342 and PI is always similar to that of living cells with the only addition of Hoechst 33342 and PI.

4.2.1. Screening of Hypervalent Iodine Reagents (1)

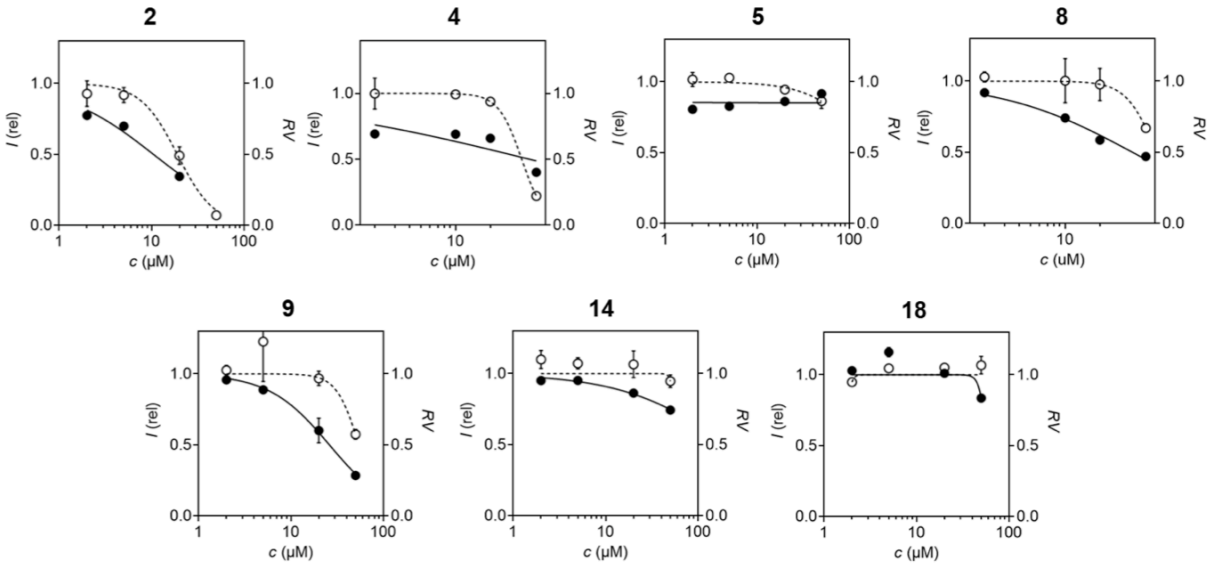

Figure S1. Automatically analyzed HCHT profiles showing fluorescence intensity (filled symbols) and relative viability (empty symbols) of HeLa cells after pre-incubation with each compound for 30 min followed by co-incubation with **26** (10 μM) for 30 min.

Table S1. Inhibition assay of thiol-mediated cellular uptake

Cpd	t_{pre}[a] (h)	t_{inc}[b] (h)	MIC[c] (μM)	IC_{50}[d] (μM)	n (IC_{50})[e]	GI_{50}[f] (μM)	n (GI_{50})[g]
2	1	0.5	< 2	10.5 ± 0.9	0.88 ± 0.08	19 ± 1	2.2 ± 0.4
4	1	0.5	< 2	-	-	37 ± 2	4.3 ± 0.6
5	1	0.5	< 2	> 50	-	> 50	-
8	1	0.5	4	39 ± 3	0.75 ± 0.05	62 ± 3	3.4 ± 2.5
9	1	0.5	7	26 ± 1	1.3 ± 0.1	> 50	-
14	1	0.5	21	> 50	-	> 50	-
18	1	0.5	50	> 50	-	> 50	-

[a] Pre-incubation time of HeLa cells with the compound. [b] Co-incubation time with the compound and **26** after pre-incubation[a]. [c] Minimum inhibitory concentration. [d] Half maximal

inhibitory concentration. [e] Hill coefficient for inhibition of cellular uptake. [f] Concentration causing 50% cell growth inhibition. [g] Hill coefficient for toxicity.

4.2.2. Screening of Hypervalent Iodine Reagents (2)

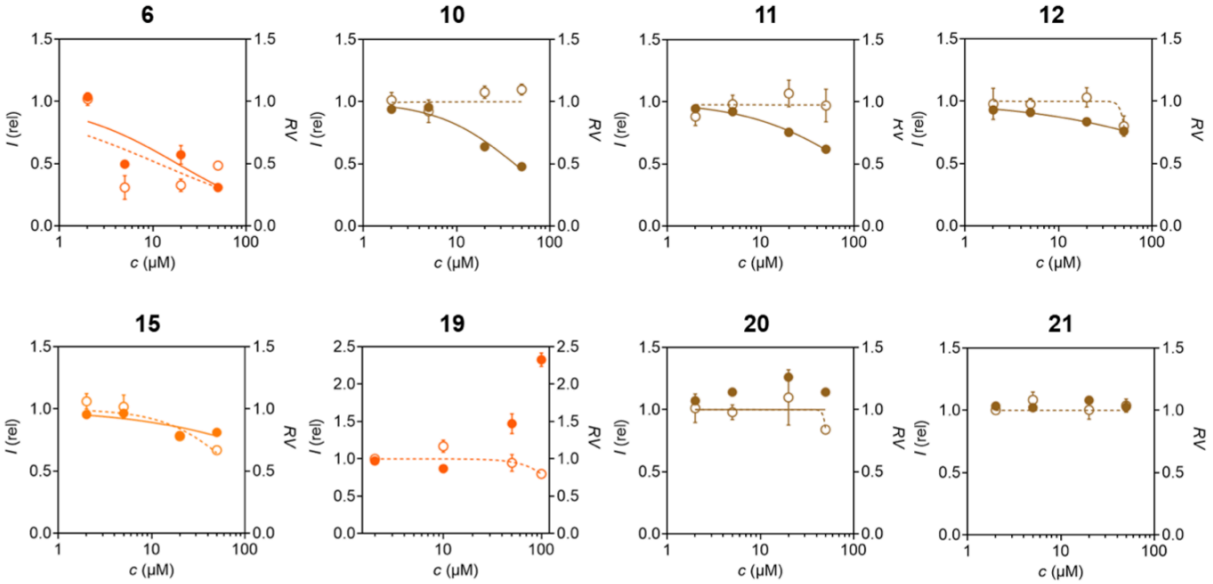

Figure S2. Automatically analyzed HCHT profiles showing fluorescence intensity (filled symbols) and relative viability (empty symbols) of HeLa cells after pre-incubation with each compound for 30 min followed by incubation with **26** (10 μM) for 30 min.

Table S2. Inhibition assay of thiol-mediated cellular uptake

Cpd	t_{pre}[a] (h)	t_{inc}[b] (h)	MIC[c] (μM)	IC_{50}[d] (μM)	n (IC_{50})[e]	GI_{50}[f] (μM)	n (GI_{50})[g]
6	1	0.5	< 2	18 ± 7	0.8 ± 0.3	12 ± 8	0.5 ± 0.3
10	1	0.5	8	42 ± 4	1.0 ± 0.1	> 50	-
11	1	0.5	10	> 50	-	> 50	-
12	1	0.5	15	> 50	-	> 50	-
15	1	0.5	21	> 50	-	> 50	-
19	1	0.5	50 [h]	-	-	> 100	-
20	1	0.5	>50	-	-	> 50	-
21	1	0.5	-	> 50	-	> 50	-

[a] Pre-incubation time of HeLa cells with the compound. [b] Co-incubation time with the compound and **26** after pre-incubation[a]. [c] Minimum inhibitory concentration. [d] Half maximal inhibitory concentration. [e] Hill coefficient for inhibition of cellular uptake. [f] Concentration causing 50% cell growth inhibition. [g] Hill coefficient for toxicity. [h] Onset of activation of uptake.

4.2.3. Screening of Other Irreversible Covalent Reagents (1)

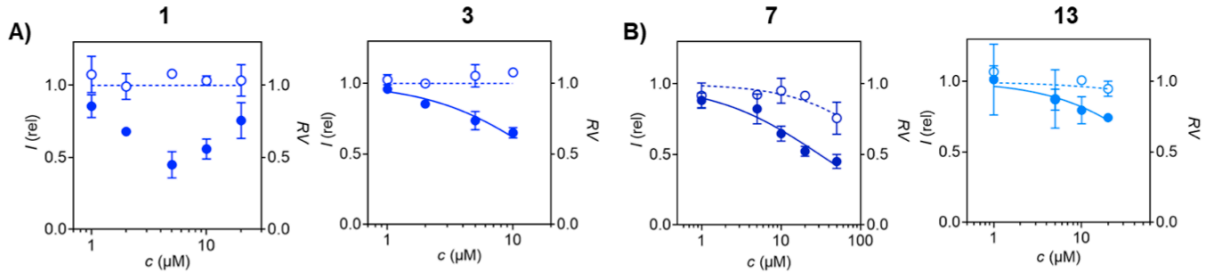

Figure S3. Automatically analyzed HCHT profiles showing fluorescence intensity (filled symbols) and relative viability (empty symbols) of HeLa cells after pre-incubation with each compound for 30 min followed by A) incubation with **26** (10 μM) for 30 min after removal of the compound; B) co-incubation with **26** (10 μM) for 30 min.

Table S3. Inhibition assay of thiol-mediated cellular uptake

Cpd	t_{pre}[a] (h)	t_{inc} (h)	MIC[d] (μM)	IC_{50}[e] (μM)	n (IC_{50})[f]	GI_{50}[g] (μM)	n (GI_{50})[h]
1	1	0.5 [b]	< 1	4.1 ± 0.5	1.1 ± 0.5	-	-
3	1	0.5 [b]	1.7	19 ± 4	0.7 ± 0.1	-	-
7	1	0.5 [c]	2.1	31 ± 6	0.7 ± 0.1	> 200	-
13	1	0.5 [c]	18.6	-	-	-	-

[a] Pre-incubation time of HeLa cells with the compound. [b] Incubation time with **26** after removal the compound after pre-incubation[a]. [c] Co-incubation time with the compound and **26** after pre-incubation[a]. [d] Minimum inhibitory concentration. [e] Half maximal inhibitory concentration. [f] Hill coefficient for inhibition of cellular uptake. [g] Concentration causing 50% cell growth inhibition. [h] Hill coefficient for toxicity.

4.2.4. Screening of Other Irreversible Covalent Reagents (2)

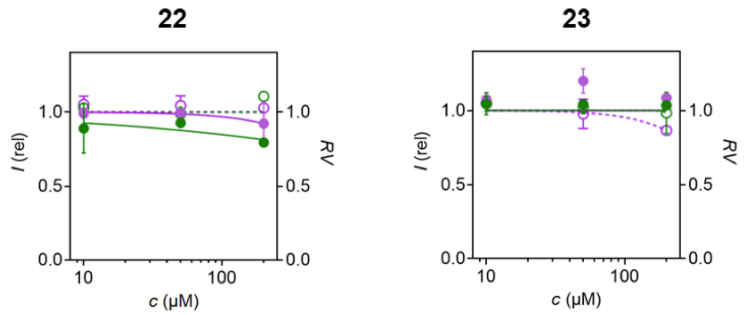

Figure S4. Automatically analyzed HCHT profiles showing fluorescence intensity (filled symbols) and relative viability (empty symbols) of HeLa cells after pre-incubation with **22** and **23** for 30 min (purple circles) and 1 h (green circles) followed by incubation with **26** (10 µM) for 30 min.

Table S4. Inhibition assay of thiol-mediated cellular uptake

Cpd	t_{pre}[a] (h)	t_{inc}[b] (h)	MIC[c] (µM)	IC_{50}[d] (µM)	n (IC_{50})[e]	GI_{50}[f] (µM)	n (GI_{50})[g]
22	0.5	0.5	> 200	-	-	> 200	-
	1	0.5	100	-	-	> 200	-
23	0.5	0.5	> 200	-	-	> 200	-
	1	0.5	> 200	-	-	> 200	-

[a] Pre-incubation time of HeLa cells with the compound. [b] Incubation time with **26** after removal the compound after pre-incubation[a]. [c] Co-incubation time with the compound and **26** after pre-incubation[a]. [d] Minimum inhibitory concentration. [e] Half maximal inhibitory concentration. [gf] Concentration causing 50% cell growth inhibition. [g] Hill coefficient for toxicity.

4.3. Cell Viability

HeLa Kyoto cells were seeded with 100 µL of cell suspension at 8.0 ×10^4 cells/mL in FluoroBrite DMEM + 10% FBS on 96-well culture plate and kept at 37 °C with 5% CO_2 for 24 h. After removing the medium, the cells were treated with 100 µL of covalent inhibitors at various concentration (0.1, 1, 5, 10, 20 and 50 µM) at 37 °C with 5% CO_2 for 48 h. Then, 20 µL of MTS solution (CellTiter-Blue®, Promega) were added to each well and the cells were incubated at 37 °C with 5% CO_2 for 0.5 h. The fluorescence of the resulting solution was recorded (ex. 560 nm / em. 590 nm).

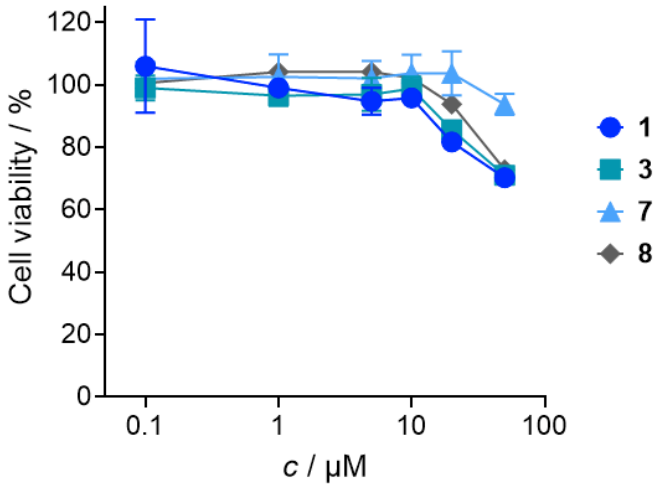

Figure S5. Cell viability by MTT assay. HeLa Kyoto cells were treated with different concentrations of compound **1**, **3**, **7** and **8** for 48 h.

5. Supporting References

[S1] L. Zong, E. Bartolami, D. Abegg, A. Adibekian, N. Sakai, S. Matile, 'Epidithiodiketopiperazines: Strain-Promoted Thiol-Mediated Cellular Uptake at the Highest Tension', *ACS Cent. Sci*. **2017**, *3*, 449-453.

[S2] J. P Brand, C. Chevalley, R. Scopelliti, J. Waser, 'Ethynyl Benziodoxolones for the Direct Alkynylation of Heterocycles: Structural Requirement, Improved Procedure for Pyrroles, and Insights into the Mechanism', *Chem. Eur. J.* **2012**, *18*, 5655-5666.

[S3] P. Eisenberger, S. Gischig, A. Togni, 'Novel 10-I-3 'Hypervalent Iodine-Based Compounds for Electrophilic Trifluoromethylation', *Chem. Eur. J.* **2006**, *12*, 2579-2586

[S4] S. G. E. Amos, S. Nicolai, J. Waser, 'Photocatalytic Umpolung of *N*- and *O*-Substituted Alkenes for the Synthesis of 1,2-Amino Alcohols and Diols', *Chem. Sci.* **2020**, *11*, 11274-11279.

[S5] F. Rodier, M. Rajzmann, J.-L. Parrain, G. Chouraqui, L. Commeiras, 'Diastereoselective Access to Polyoxygenated Polycyclic Spirolactones through a Rhodium-Catalyzed [3+2] Cycloaddition Reaction: Experimental and Theoretical Studies', *Chem. Eur. J.* **2013**, *19*, 2467-2477.

[S6] A. Berkessel, J. Kramer, F. Mummy, J. M. Neudorfl, R. Haag, 'Dendritic Fluoroalcohols as Catalysts for Alkene Epoxidation with Hydrogen Peroxide', *Angew. Chem. Int. Ed.* **2013**, *52*, 739-743.

[S7] R. Frei, M. D. Wodrich, D. P. Hari, P.-A. Borin, C. Chauvier, J. Waser, 'Fast and Highly Chemoselective Alkynylation of Thiols with Hypervalent Iodine Reagents Enabled through a Low Energy Barrier Concerted Mechanism', *J. Am. Chem. Soc.* **2014**, *136*, 16563-16573.

[S8] L. Díaz, J. Bujons, J. Casas, A. Llebaria, A. Delgadob, 'Click Chemistry Approach to New N-Substituted Aminocyclitols as Potential Pharmacological Chaperones for

Gaucher Disease', *J. Med. Chem.* **2010**, *53*, 5248-5255.

[S9] D. Abegg, R. Frei, L. Cerato, D. P. Hari, C. Wang, J. Waser, A. Adibekian, 'Proteome-Wide Profiling of Targets of Cysteine Reactive Small Molecules by Using Ethynyl Benziodoxolone Reagents', *Angew. Chem. Int. Ed.* **2015**, *54*, 10852-10857.

[S10] A.-L. Barthelemy, V. Certal, G. Dagousset, E. Anselmi, L. Bertin, L. Fabien, B. Salgues, P. Courtes, C. Poma, Y. El-Ahmad, E. Magnier, 'Optimization and Gram-Scale Preparation of S-Trifluoromethyl Sulfoximines and Sulfilimino Iminiums, Powerful Reagents for the Late Stage Introduction of the CF_3 Group', *Org. Process Res. Dev.* **2020**, *24*, 704-712.

[S11] J. Kalim, T. Duhail, T.-N. Le, N. Vanthuyne, E. Anselmi, A. Togni, E. Magnier, 'Merging Hypervalent Iodine and Sulfoximine Chemistry: a New Electrophilic Trifluoromethylation Reagent', *Chem. Sci.* **2019**, *10*, 10516-10523.

[S12] E. Le Du, T. Duhail, M. D. Wodrich, R. Scopelliti, F. Fadaei-Tirani, E. Anselmi, E. Magnier, J. Waser, 'Structure and Reactivity of *N*-Heterocyclic Alkynyl Hypervalent Iodine Reagents', *Chem. Eur. J.* **2021**, DOI: https://doi.org/10.1002/chem.202101475.

[S13] R. Tessier, R. K. Nandi, B. G. Dwyer, D. Abegg, C. Sornay, J. Ceballos, S. Erb, S. Cianférani, A. Wagner, G. Chaubet, A. Adibekian, J. Waser, 'Ethynylation of Cysteine Residues: From Peptides to Proteins in Vitro and in Living Cells', *Angew. Chem., Int. Ed.* **2020**, *59*, 10961-10970.

[S14] D. P. Hari, L. Schouwey, V. Barber, R. Scopelliti, F. Fadaei-Tirani, J. Waser, 'Ethynylbenziodazolones (EBZ) as Electrophilic Alkynylation Reagents for the Highly Enantioselective Copper-Catalyzed Oxyalkynylation of Diazo Compounds', *Chem. Eur. J.* **2019**, *25*, 9522-9528.

[S15] S. Dalai, V. N. Belov, S. Nizamov, K. Rauch, D. Finsinger, A. de Meijere, 'Access to Variously Substituted 5,6,7,8-Tetrahydro-3*H*-quinazolin-4-ones via Diels–Alder Adducts

of Phenyl Vinyl Sulfone to Cyclobutene-Annelated Pyrimidinones', *Eur. J. Org. Chem.* **2006**, 2753-2765.

[S16] T. Yao, 'Facile *N*-Arylation of Amidines and *N,N*-Disubstituted Amidines', *Tetrahedron Lett.* **2015**, *56*, 4623-4626.

[S17] E. Stridfeldt, A. Seemann, M. J. Bouma, C. Dey, A. Ertan, B. Olofsson, 'Synthesis, Characterization and Unusual Reactivity of Vinylbenziodoxolones-Novel Hypervalent Iodine Reagents', *Chem. Eur. J*. **2016**, *22*, 16066-16070.

[S18] E. F. Perozzi, R. S. Michalak, G. D. Figuly, W. H. Stevenson, D. Dess, M. R. Ross, J. C. Martin, 'Directed Dilithiation of Hexafluorocumyl Alcohol Formation of a Reagent for the Facile Introduction of a Stabilizing Bidentate Ligand in Compounds of Hypervalent Sulfur (10-S-4), Phosphorus (10-P-5), Silicon (10-Si-5), and Iodine (10-I-3)', *J. Org. Chem.* **1981**, *46*, 1049-1053.

[S19] J. Cvengros, D. Stolz, A. Togni, 'A Concise Synthesis of *ortho*-Iodobenzyl Alcohols via Addition of *ortho*-Iodophenyl Grignard Reagent to Aldehydes and Ketones', *Synthesis* **2009**, 2818-2824.

[S20] A. J. Blake, A. Novak, M. Davies, R. I. Robinson, S. Woodward, 'Preparation of 1,1′-Oxy-Bis(3,3-Bis(Trifluoromethyl)-3(1*H*)-1,2-Benziodoxole) and 2-(*N*-(*p*-Toluenesulfonyl)imino)iodobenzylmethyl Ether', *Synth. Commun.* **2009**, *39*, 1065-1075.

[S21] a) T. Harschneck, S. Hummel, S. Kirsch, P. Klahn, 'Practical Azidation of 1,3-Dicarbonyls', *Chem. Eur. J.* **2012**, *18*, 1187-1193; b) A. Bredenkamp, F. Mohr, S. Kirsch, 'Synthesis of Isatins through Direct Oxidation of Indoles with IBX-SO_3K/Na', *Synthesis*, **2015**, *47*, 1937-1943.

[S22] J. Ceballos, E. Grinhagena, G. Sangouard, C. Heinis, J. Waser, 'Cys–Cys and Cys–Lys Stapling of Unprotected Peptides Enabled by Hypervalent Iodine Reagents', *Angew. Chem., Int. Ed.* **2021**, *60*, 9022-9031.

[S23] M. Chen, Z. T. Huang, Q. Y. Zheng, 'Organic Base-Promoted Enantioselective Electrophilic Cyanation of β-Keto Esters by Using Chiral Phase-Transfer Catalysts', *Org. Biomol. Chem.* **2015**, *13*, 8812-8816.

[S24] A. Kommreddy, M. S. Bowsher, M. R. Gunna, K. Botha, T. K. Vinod, 'Expedient Synthesis and Solvent Dependent Oxidation Behavior of a Water-Soluble IBX Derivative', *Tetrahedron Lett.* **2008**, *49*, 4378-4382.

[S25] A. K. Mishra, R. Tessier, D. P. Hari, J. Waser, 'Amphiphilic Iodine(III) Reagents for the Lipophilization of Peptides in Water', *Angew. Chem. Int. Ed.* **2021**, doi.org/10.1002/anie.202106458.

[S26] L. J. Macpherson, A. E. Dubin, M. J. Evans, F. Marr, P. G. Schultz, B. F. Cravatt, A. Patapoutian, 'Noxious Compounds Activate TRPA1 Ion Channels Through Covalent Modification of Cysteines', *Nature* **2007**, *445*, 541-545.

[S27] C. Zambaldo, E. V. Vinogradova, X. Qi, J. Iaconelli, R. M. Suciu, M. Koh, K. Senkane, S. R. Chadwick, B. B. Sanchez, J. S. Chen, A. K. Chatterjee, P. Liu, P. G. Schultz, B. F. Cravatt, M. J. Bollong, '2-Sulfonylpyridines as Tunable, Cysteine-Reactive Electrophiles', *J. Am. Chem. Soc.* **2020**, *142*, 8972-8979.

[S28] H. F. Motiwala, Y.-H. Kuo, B. L. Stinger, B. A. Palfey, B. R. Martin, 'Tunable Heteroaromatic Sulfones Enhance in-Cell Cysteine Profiling'. *J. Am. Chem. Soc.* **2020**, *142*, 1801-1810.

[S29] J. H. Kim, Y. Chung, H. Jeon, S. Lee, S. Kim, 'Stereoselective Asymmetric Synthesis of Pyrrolidines with Vicinal Stereocenters Using a Memory of Chirality-Assisted Intramolecular S_N2' Reaction', *Org. Lett.* **2020**, *22*, 3989-3992.

[S30] Y. Cheng, A.-T. Pham, T. Kato, B. Lim, D. Moreau, J. López-Andarias, L. Zong, N. Sakai, S. Matile, 'Inhibitors of Thiol-Mediated Uptake', *Chem. Sci.* **2021**, *12*, 626–631.

The original data can be found at: https://dx.doi.org/10.5281/zenodo.4974210

6. NMR Spectra

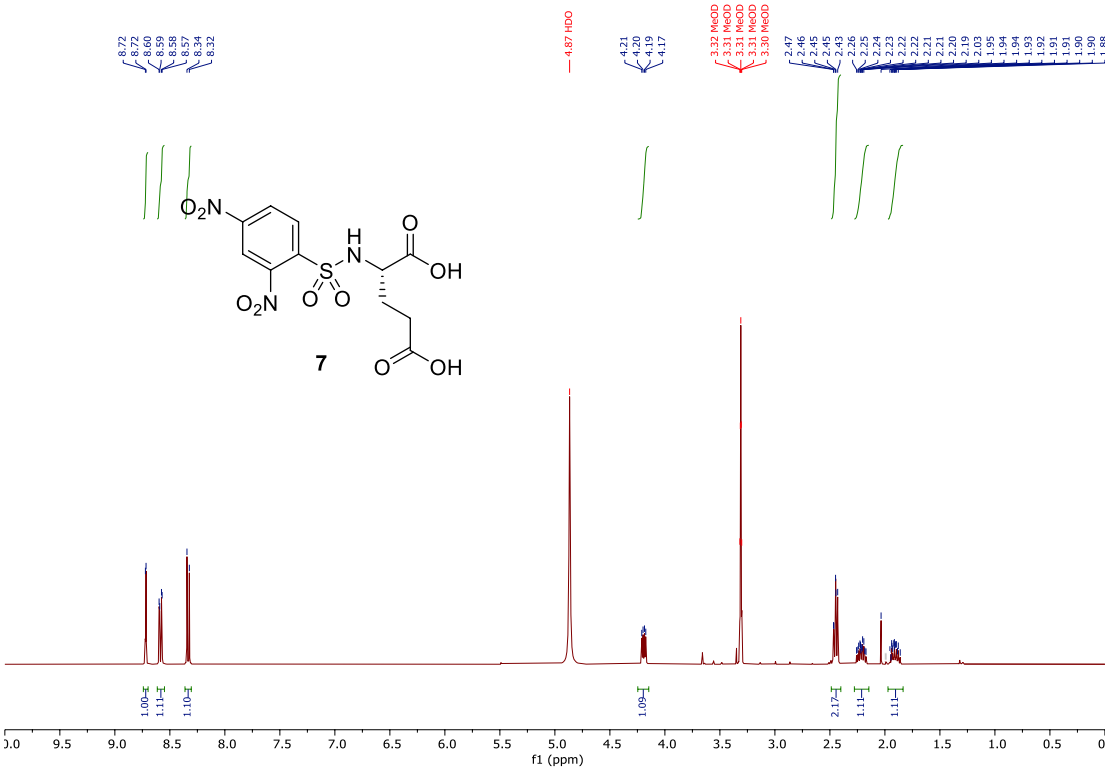

Figure S6. 400 MHz ^{1}H NMR spectrum of **7** in CD_3OD.

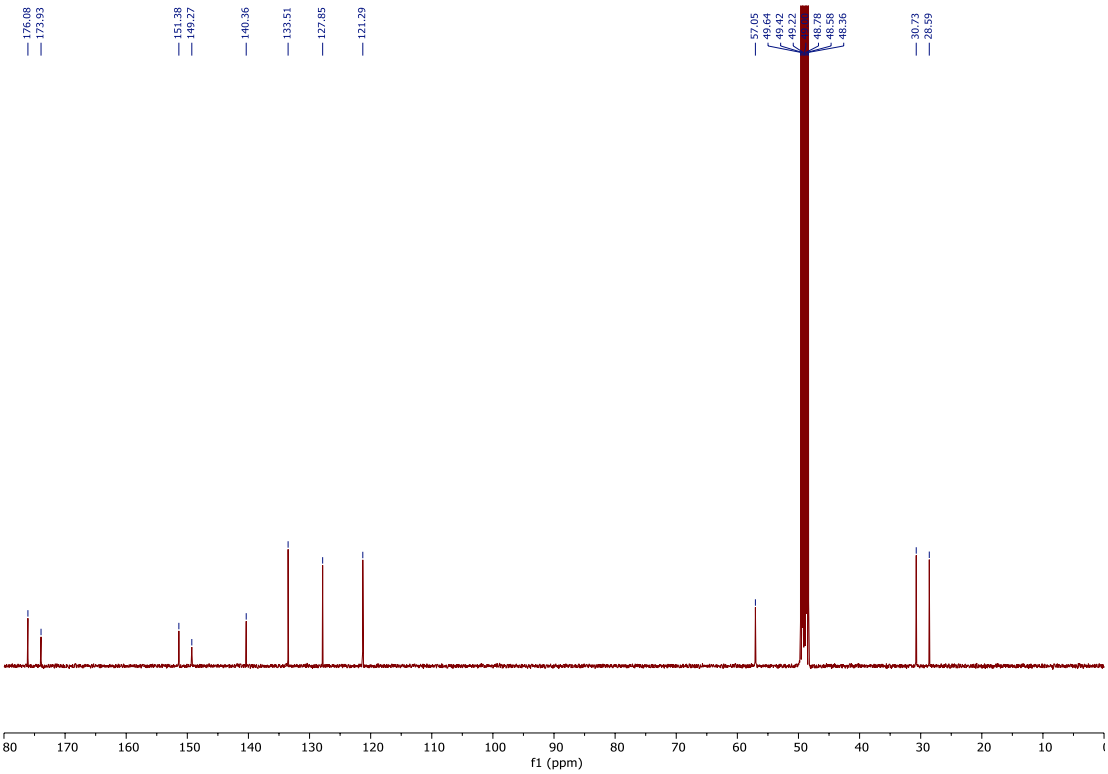

Figure S7. 101 MHz ^{13}C NMR spectrum of **7** in CD_3OD.

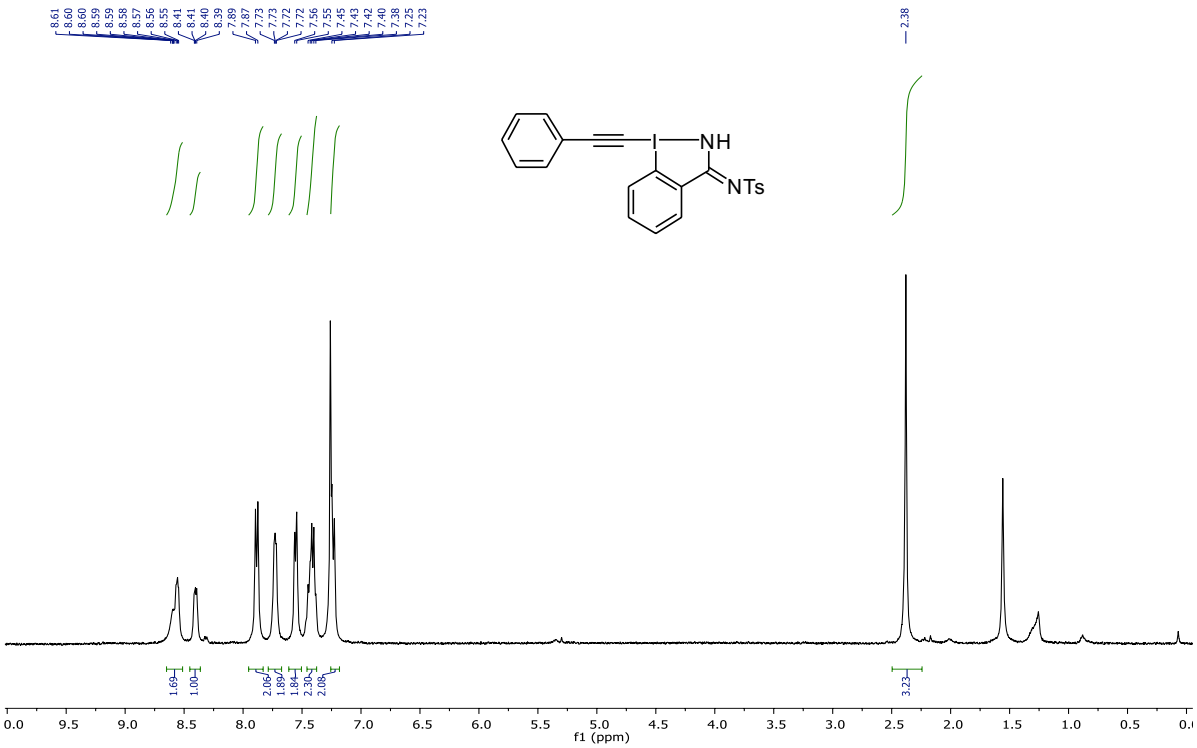

Figure S8. 400 MHz ^{1}H NMR spectrum of **10** in $CDCl_3$.

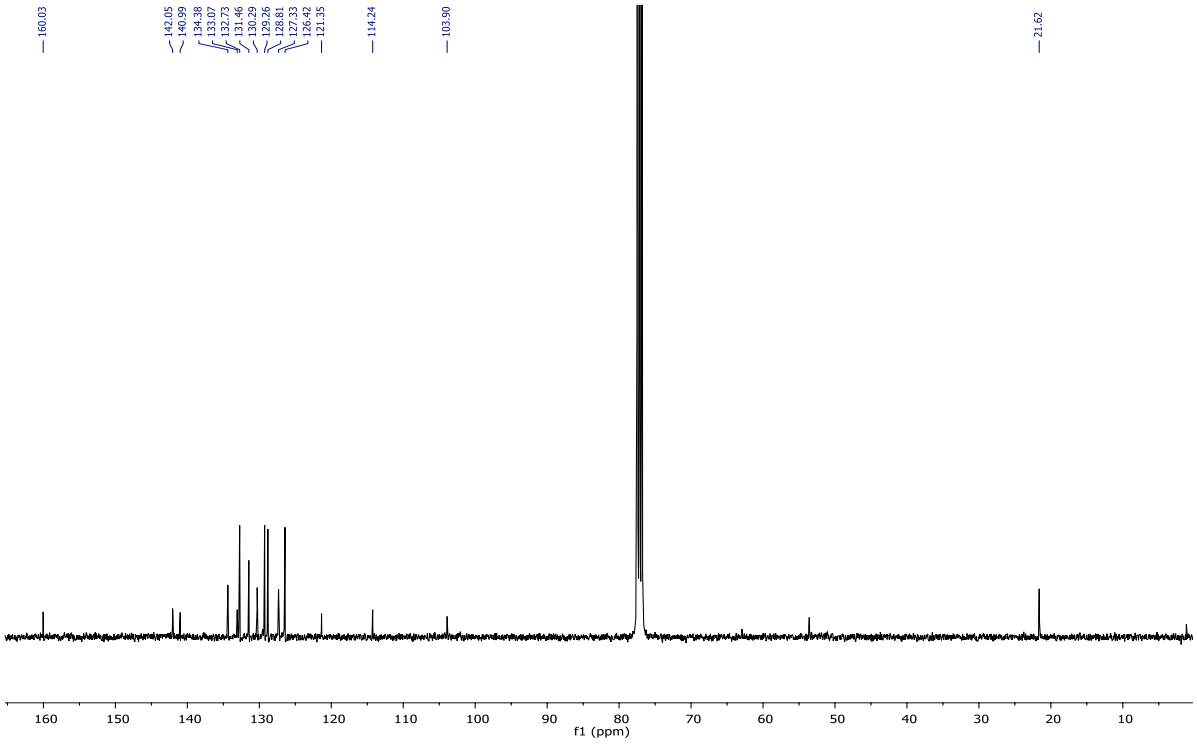

Figure S9. 101 MHz ^{13}C NMR spectrum of **10** in $CDCl_3$.

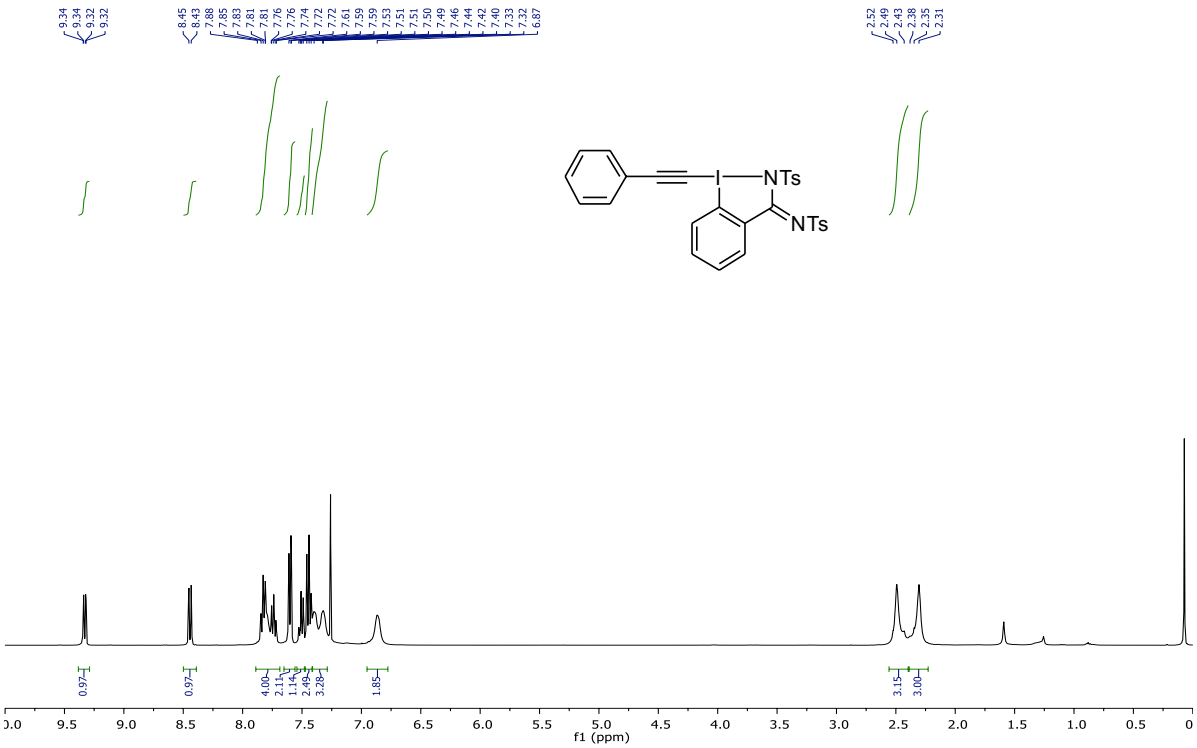

Figure S10. 400 MHz ^{1}H NMR spectrum of **21** in $CDCl_3$.

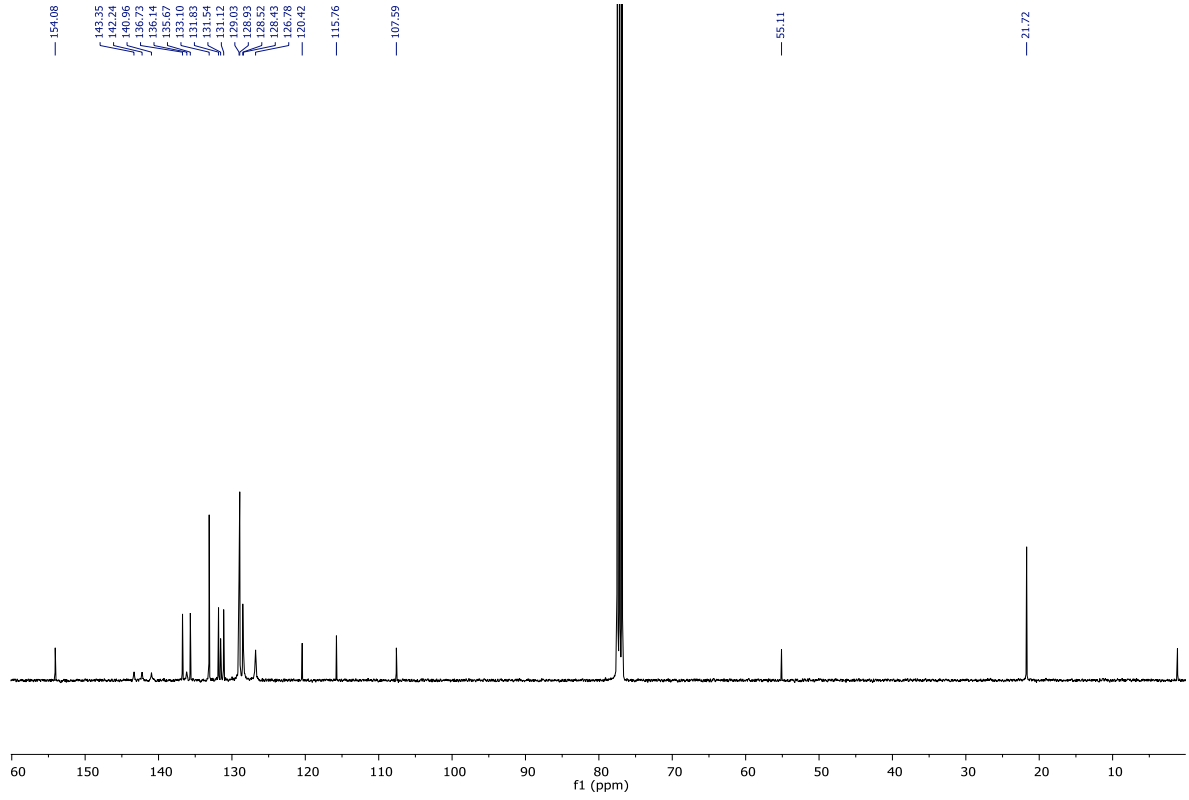

Figure S11. 101 MHz ^{13}C NMR spectrum of **21** in $CDCl_3$.